1997. The TEL gene products: nuclear phosphoproteins with DNA binding properties. Oncogene **14**:349–357.
27. **Potter, M. D., A. Buijs, B. Kreider, L. van Rompaey, and G. Grosveld.** 2000. Identification and characterization of a new human ETS-family transcription factor, TEL2, that is expressed in hematopoietic tissues and can associate with *TEL1/ETV6*. Blood **95**:3341–3348.
28. **Rabault, B., M. F. Roussel, C. T. Quang, and J. Ghysdael.** 1996. Phosphorylation of Ets1 regulates the complementation of a CSF-1 receptor impaired in mitogenesis. Oncogene **13**:877–881.
29. **Slupsky, C. M., L. N. Gentile, L. W. Donaldson, C. D. Mackereth, J. J. Seidel, B. J. Graves, and L. P. McIntosh.** 1998. Structure of the Ets-1 pointed domain and mitogen-activated protein kinase phosphorylation site. Proc. Natl. Acad. Sci. USA **95**:12129–12134.
30. **Tanaka, T., M. Kurokawa, K. Ueki, K. Tanaka, Y. Imai, K. Mitani, K. Okazaki, N. Sagata, Y. Yazaki, Y. Shibata, T. Kadowaki, and H. Hirai.** 1996. The extracellular signal-regulated kinase pathway phosphorylates AML1, an acute myeloid leukemia gene product, and potentially regulates its transactivation ability. Mol. Cell. Biol. **16**:3967–3979.
31. **Ueki, K., S. Matsuda, K. Tobe, Y. Gotoh, H. Tamemoto, M. Yachi, Y. Akanuma, Y. Yazaki, E. Nishida, and T. Kadowaki.** 1994. Feedback regulation of mitogen-activated protein kinase kinase activity of c-Raf-1 by insulin and phorbol ester stimulation. J. Biol. Chem. **269**:15756–15761.
32. **Van Rompaey, L., M. Potter, C. Adams, and G. Grosveld.** 2000. Tel induces a G1 arrest and suppresses Ras-induced transformation. Oncogene **19**:5244–5250.
33. **Waga, K., Y. Nakamura, K. Maki, H. Arai, T. Yamagata, K. Sasaki, M. Kurokawa, H. Hirai, and K. Mitani.** 2003. Leukemia-related transcription factor TEL accelerates differentiation of Friend erythroleukemia cells. Oncogene **22**:59–68.
34. **Wang, L., and S. W. Hiebert.** 2001. TEL contacts multiple co-repressors and specifically associates with histone deacetylase-3. Oncogene **20**:3716–3725.
35. **Wang, L. C., F. Kuo, Y. Fujiwara, D. G. Gilliland, T. R. Golub, and S. H. Orkin.** 1997. Yolk sac angiogenesis defect and intra-embryonic apoptosis in mice lacking the Ets-related factor TEL. EMBO J. **16**:4374–4383.
36. **Wang, L. C., W. Swat, Y. Fujiwara, L. Davidson, J. Visvader, F. Kuo, F. W. Alt, D. G. Gilliland, T. R. Golub, and S. H. Orkin.** 1998. The *TEL/ETV6* gene is required specifically for hematopoiesis in the bone marrow. Genes Dev. **12**:2392–2402.
37. **Witt, O., K. Sand, and A. Pekrun.** 2000. Butyrate-induced erythroid differentiation of human K562 leukemia cells involves inhibition of ERK and activation of p38 MAP kinase pathways. Blood **95**:2391–2396.
38. **Yang, B. S., C. A. Hauser, G. Henkel, M. S. Colman, C. van Beveren, K. J. Stacey, D. A. Hume, R. A. Maki, and M. C. Ostrowski.** 1996. Ras-mediated phosphorylation of a conserved threonine residue enhances the transactivation activities of c-Ets1 and c-Ets2. Mol. Cell. Biol. **16**:538–547.
39. **Yang, S. H., A. Galanis, and A. D. Sharrocks.** 1999. Targeting of p38 mitogen-activated protein kinases to MEF2 transcription factors. Mol. Cell. Biol. **19**:4028–4038.

Correspondence

To the editor:

SCL/Tal1 and lymphoid versus myeloid lineage assignment

In their recent paper, Kunisato et al[1] describe the role of stem cell leukemia gene (SCL) in regulating lineage fate in hematopoietic stem cells. Their experiments involve retroviral expression of SCL and a "dominant-negative" mutant of SCL (DN-SCL) in hematopoietic stem cells and their progeny. They propose that levels of SCL regulate lineage commitment: enforced expression of SCL favored myeloid differentiation, while expression of the DN-SCL favored lymphoid differentiation. We query the interpretation of the results obtained with the DN-SCL mutant, as its design and effects are not suggestive of a specific dominant-negative function. The authors cite Aplan et al[2] and Krosl et al[3] for the design of the dominant-negative SCL. In these papers the basic domain of SCL was deleted. This mutant is unable to bind to DNA, however, heterodimerization with E2A proteins remains intact through the presence of the helix-loop-helix (HLH) domain. The DN-SCL mutant used by Kunisato et al[1] lacks both the basic and HLH domains. Such a mutant would be predicted to abrogate not only DNA binding, but also the ability to interact with E2A proteins. The remaining N- and C-terminal portions of SCL have no known function—indeed, a truncation mutant comprising only the basic and HLH domains could rescue hematopoiesis of SCL-null embryonic stem cells,[4] suggesting that the N- and C-terminal amino acids are not essential. Since a dominant-negative mutant usually relies on deletion of specific functional domains while retaining vital protein interactions, it is difficult to understand how this mutant could act as a dominant negative. Moreover, enforced expression of the DN-SCL only mildly affects erythroid cell production in vitro or in vivo (Figures 3 and 7), whereas loss of SCL by conditional deletion has demonstrated that SCL is essential for erythroid burst-forming units (BFU-E) and production of red cells in vivo.[5-7] Thus, there is no available data to positively suggest that the DN-SCL used by Kunisato and colleagues[1] inhibits the function of SCL. Nonetheless, it is possible that the N- and C-terminal portions of SCL have an unknown function that causes the observed effects on lineage specification. However, without the correct controls, such as rescue of the DN-SCL effect with wild-type SCL, it is impossible to discriminate specific from nonspecific effects. In light of this and since the effects on myeloid and lymphoid lineage output are subtle and transient, it is important to regard with caution the assertion that the effects are due to a dominant-negative effect on SCL.

Mark Hall and David Curtis

Correspondence: Mark Hall, Rotary Bone Marrow Research Laboratory, Royal Melbourne Hospital, Parkville, Victoria 3050, Australia; e-mail: hall@wehi.edu.au.

References

1. Kunisato A, Chiba S, Saito T, et al. Stem cell leukemia protein directs hematopoietic stem cell fate. Blood. 2004;103:3336-3341.
2. Aplan PD, Nakahara K, Orkin SH, Kirsch IR. The SCL gene product: a positive regulator of erythroid differentiation. EMBO J. 1992;11:4073-4081.
3. Krosl G, He G, Lefrancois M, et al. Transcription factor SCL is required for c-kit expression and c-Kit function in hemopoietic cells. J Exp Med. 1998;188:439-450.
4. Porcher C, Liao EC, Fujiwara Y, Zon LI, Orkin SH. Specification of hematopoietic and vascular development by the bHLH transcription factor SCL without direct DNA binding. Development. 1999;126:4603-4615.
5. Mikkola HK, Klintman J, Yang H, et al. Haematopoietic stem cells retain long-term repopulating activity and multipotency in the absence of stem-cell leukaemia SCL/tal-1 gene. Nature. 2003;421:547-551.
6. Hall MA, Curtis DJ, Metcalf D, et al. The critical regulator of embryonic hematopoiesis, SCL, is vital in the adult for megakaryopoiesis, erythropoiesis, and lineage choice in CFU-S12. Proc Natl Acad Sci U S A. 2003;100:992-997.
7. Curtis DJ, Hall MA, Van Stekelenburg LJ, Robb L, Jane SM, Begley CG. SCL is required for normal function of short-term repopulating hematopoietic stem cells. Blood. 2004;103:3342-3348.

Response:

Dominant-negative activity of stem cell leukemia (SCL) lacking bHLH domain

Queries from Hall and Curtis on our paper[1] in *Blood* include some important issues. As they argue, the construct of interest (ΔbHLH SCL) may not have an ability to interact with E2A proteins. Indeed, our experiment showed that it does not interact with wild-type (WT) stem cell leukemia (SCL) (data not shown). However, this does not imply that ΔbHLH SCL consisting only of the N- and C-terminal portions of SCL does not have any function. Contrary to the argument by Porcher et al,[2] their results could indicate that the N- and C-terminal portions of SCL have some roles, since it appears that the bHLH domain alone does not completely rescue the SCL-null phenotype. In addition, as was described in our paper (Figure 7), we found maturation arrest in the erythroid progenitors by introducing ΔbHLH SCL. This observation is considered to be biologic evidence of dominant-negative effect of ΔbHLH SCL on wild-type SCL, given the phenotype of SCL conditional knockout mice.[3] In this regard, we are afraid that the questioners may misunderstand our description in the paper.

To explore the proteins that interact with ΔbHLH SCL, we have performed a coprecipitation analysis (Figure 1). We transfected HEK293 peak cells with plasmids containing FLAG-tagged WT SCL and ΔbHLH SCL under the cytomegalovirus (CMV) promoter. Two days after the transfection, lysates were prepared and immunoprecipitated with the anti-FLAG antibody-coated beads (Sigma, St Louis, MO). The samples then were resolved through sodium dodecyl sulfate–polyacrylamide gel electrophoresis (SDS-PAGE), and the gel was silver-stained (Dai-ichi Kagaku, Tokyo, Japan). We found that some proteins coprecipitated commonly with WT SCL and ΔbHLH SCL (solid arrows), and others coprecipitated with WT SCL alone (dotted arrows). It is possible that the commonly precipitated proteins

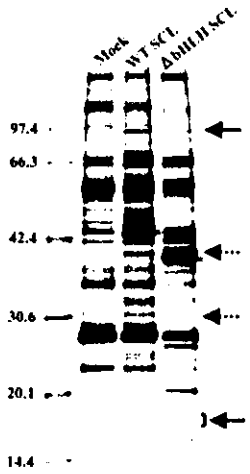

Figure 1. Proteins co-precipitated with WTSCL or ΔbHLH SCL. WT SCL and ΔbHLH SCL are indicated by asterisks. The bands indicated by arrows are reproducibly precipitated.

interact with the N- or C-terminal region of SCL, and thus, it is speculated that ΔbHLH SCL functions against WT SCL through the competition for binding to these proteins. To further explore the underlying biochemical mechanisms, we have sequenced some of these coprecipitated proteins, which we hope will be reported in the near future.

We disagree with the comment by the questioners that we should be able to show the rescue of the effect of ΔbHLH SCL with WT SCL. This is not an appropriate experiment to show the dominant-negative effect of ΔbHLH SCL.

Although the biochemical mechanisms need to be further disclosed, clear are our findings on the distinct biologic functions of WT SCL and ΔbHLH SCL on the commitment fate determination of hematopoietic stem cells. We hope that our ongoing study will give a clear answer to the mechanisms for how ΔbHLH SCL functions in a dominant-negative fashion against WT SCL.

Atsushi Kunisato, Seishi Ogawa, and Shigeru Chiba

Correspondence: Shigeru Chiba, Department of Cell Therapy and Transplantation Medicine, University of Tokyo Hospital 7-3-1, Hongo, Bunkyo-ku, Tokyo; e-mail: schiba-tky@umin.ac.jp.

References

1. Kunisato A, Chiba S, Saito T, et al. Stem cell leukemia protein directs hematopoietic stem cell fate. Blood. 2004;103:3336-3341.
2. Porcher C, Liao EC, Fujiwara Y, Zon LI, Orkin SH. Specification of hematopoietic and vascular development by the bHLH transcription factor SCL without direct DNA binding. Development. 1999;126:4603-4615.
3. Mikkola HK, Klintman J, Yang H, et al. Haematopoietic stem cells retain long-term repopulating activity and multipotency in the absence of stem-cell leukaemia SCL/tal-1 gene. Nature. 2003;421:547-551.

To the editor:

Potential curability of newly diagnosed acute promyelocytic leukemia without use of chemotherapy: the example of liposomal all-*trans* retinoic acid

Several years ago we reported that liposomal all-*trans* retinoic acid (L-ATRA) used alone might cure some patients with untreated acute promyelocytic leukemia (APL).[1,2] The median follow-up was 1.5 years from complete remission (CR) date. Because the risk of relapse does not decrease appreciably until considerably later,[3] we herein update the study. The L-ATRA dose was 90 mg/m^2 every other day until CR, after which this dose was given 3 times weekly for 9 months. Using a sensitivity level of 10 (−4), polymerase chain reaction (PCR) testing for the promyelocytic leukemia/retinoic acid receptor{alpha} (PML-RAR) (fusion protein) was done every 3 months for 2 years from CR date. If positive, the test was repeated 2 to 4 weeks later. If again positive ("molecular relapse"), patients received 12 mg/m^2 idarubicin 3 times daily every 4 to 5 weeks for 3 courses. Thirty-four patients, median age 49 years, median white blood cell count (WBC) 2000/μL, were treated: 8 were high risk (WBC count > 10 000/μL) using Sanz et al's system.[4] The CR rate was 26 of 34, but only 3 of 8 in high-risk patients. Of the 34 patients, 10 (29%, 95% CI 15%-47%) remain alive in first CR at a median of 4.5 years (range, 3.0-5.5 years) from CR date despite never receiving other anti-APL therapy. In each case, the most recent PCR test is negative, having been obtained a median of 3.2 years (range, 1.4-5.5 years) years from CR date. The remaining 16 patients who entered CR received idarubicin; in one of these, the reports of the relevant PCRs were later changed to negative and in another only a single PCR test was positive. Thus, 14 patients "required" idarubicin: 8 had molecular relapse (at a median of 9 months from CR date), 2 failed to achieve molecular CR despite 6 months of L-ATRA monotherapy, and 4 had simultaneous clinical and molecular relapse (at a median of 17 months from CR date). The 10 patients who never received treatment other than L-ATRA each had a presenting WBC count less than 10 000/μL, as did 13 of the 14 who required idarubicin. The 2 groups also had similar distributions of initial WBC count, platelet count, and type of PML-RAR (isoform and age). The PCR status at CR was of no discriminatory value since all patients but one were PCR positive at CR, with 24 of 26 becoming negative by 3 months. Of the 10 patients whose first indication of failure was molecular, 9 received idarubicin in (hematologic) CR. Of those, 6 remain in hematologic CR, while 3 had hematologic relapse, which occurred within 1 year of molecular failure.

The immediate significance of our results is limited. L-ATRA is unavailable commercially. The 3 of 8 CR rate in high-risk patients seems extraordinarily low. Furthermore, while possibly sparing two fifths (ie, 10 of 26) of low-risk patients the need for chemotherapy, L-ATRA was not free of toxicity[1,2] and required 3 intravenous infusions weekly. Nonetheless, the observation that patients can be potentially cured of APL without use of chemotherapy should encourage further attempts in the same direction as, for example, in our current trial using ATRA and arsenic trioxide.[5]

Functional Domains of Runx1 Are Differentially Required for CD4 Repression, TCRβ Expression, and CD4/8 Double-Negative to CD4/8 Double-Positive Transition in Thymocyte Development[1]

Masahito Kawazu,*† Takashi Asai,* Motoshi Ichikawa,* Go Yamamoto,* Toshiki Saito,* Susumu Goyama,* Kinuko Mitani,¶ Kohei Miyazono,† Shigeru Chiba,*‡ Seishi Ogawa,*§ Mineo Kurokawa,[2]* and Hisamaru Hirai*‡

Runx1 (AML1) has multiple functions in thymocyte development, including CD4 repression in immature thymocytes, expression of TCRβ, and efficient β-selection. To determine the functional domains of Runx1 important for thymocyte development, we cultured Runx1-deficient murine fetal liver (FL) cells on OP9-Delta-like 1 murine stromal cells, which express Delta-like 1 and support thymocyte development in vitro, and introduced Runx1 or C-terminal-deletion mutants of Runx1 into the FL cells by retrovirus infection. In this system, Runx1-deficient FL cells failed to follow normal thymocyte development, whereas the introduction of Runx1 into the cells was sufficient to produce thymocyte development that was indistinguishable from that in wild-type FL cells. In contrast, Runx1 mutants that lacked the activation domain necessary for initiating gene transcription did not fully restore thymocyte differentiation, in that it neither repressed CD4 expression nor promoted the CD4/8 double-negative to CD4/8 double-positive transition. Although the C-terminal VWRPY motif-deficient mutant of Runx1, which cannot interact with the transcriptional corepressor Transducin-like enhancer of split (TLE), promoted the double-negative to double-positive transition, it did not efficiently repress CD4 expression. These results suggest that the activation domain is essential for Runx1 to establish thymocyte development and that Runx1 has both TLE-dependent and TLE-independent functions in thymocyte development. *The Journal of Immunology,* **2005, 174: 3526–3533.**

Runx1 (also called *AML1*, *Pebpa2b*, or *Cbfa2*) encodes a member of a family of runt transcription factors that was first identified in humans as a gene that is disrupted in t(8;21) acute myeloid leukemia (1). Homozygous disruption of *Runx1* in mice revealed that Runx1 plays an essential role in definitive hematopoiesis (2, 3). Furthermore, it has been suggested from the very beginning of its cloning that Runx1 also plays roles during thymocyte development (4–6). Runx1, together with other cofactors, binds to the enhancers of *TCR*α (7), β (8), γ (9), and δ (10) and activates transcription of these genes. Runx1 is expressed during thymocyte development as demonstrated by Northern blotting, as well as in situ hybridization of mRNA (11, 12). It is mainly expressed in cortical thymocytes (13), and quantitative real-time PCR of reverse-transcribed RNA revealed that Runx1 mRNA is abundant in CD4/CD8 double-negative (DN)[3] thymocytes (14). When Runx1 was overexpressed in thymocytes using a transgenic system, it was shown to induce CD8 single-positive (SP) thymocyte differentiation (15) and to inhibit the differentiation of Th2 effector T cells (16). Recently, we found that T cell-specific disruption of *Runx1* in mice using the *Cre-loxP* recombinase system results in a profound defect in the DN to CD4/8 double-positive (DP) transition,[4] and others also demonstrated that Runx1 actively represses *CD4* expression in DN thymocytes (14). Together, these findings confirm that Runx1 plays an essential role in early thymocyte development. In view of its functions in T cell development, it is noteworthy that the *Runx1* gene is disrupted in t(4;21)(q28;q22) found in T cell acute lymphoblastic leukemia (17, 18).

Runx1 has several distinct domains of defined biochemical functions. The Runt domain mediates both binding to DNA and dimerization with core-binding factor β subunit (4), whereas the activation domain interacts with transcriptional coactivators to upregulate transcription of the target genes (19, 20). Toward the C terminus of the activation domain lies an inhibitory domain that counteracts the effect of the activation domain (21). Furthermore,

Departments of *Hematology and Oncology, †Molecular Pathology, ‡Cell Therapy and Transplantation Medicine, and §Regeneration Medicine for Hematopoiesis, Graduate School of Medicine, University of Tokyo, Tokyo, Japan; and ¶Department of Hematology, Dokkyo University School of Medicine, Tochigi, Japan

Received for publication September 22, 2004. Accepted for publication January 4, 2005.

The costs of publication of this article were defrayed in part by the payment of page charges. This article must therefore be hereby marked *advertisement* in accordance with 18 U.S.C. Section 1734 solely to indicate this fact.

[1] This work was supported in part by Grants-in-Aid for Scientific Research from KAKENHI (14370300, 13218021, 13557080, and 16·61610), Special Coordination Funds for Promoting Science and Technology from the Ministry of Education, Culture, Sports, Science and Technology, the Japanese Government, and Research on Human Genome and Tissue Engineering, Health and Labor Sciences Research Grants from the Ministry of Health, Labour and Welfare of Japan, H14-GENOME-006.

[2] Address correspondence and reprint requests to Dr. Mineo Kurokawa, Department of Hematology and Oncology, Graduate School of Medicine, University of Tokyo, 7-3-1 Hongo, Bunkyo-Ku, Tokyo 113-8655, Japan. E-mail address: kurokawa-tky@umin.ac.jp

[3] Abbreviations used in this paper: DN, double-negative; SP, single-positive; DP, double-positive; TLE, Transducin-like enhancer of split; FTOC, fetal thymus organ culture; FL, fetal liver; tg, transgenic; rh, recombinant human; cko, conditionally knocked out; ctrl, control.

[4] T. Asai, T. Yamagata, T. Saito, M. Ichikawa, S. Seo, G. Yamamoto, K. Maki, K. Mitani, H. Oda, S. Chiba, et al. Runx1 is required for integrity of the pre-T cell receptor complex and Lck kinase activity in early thymocyte development. *Submitted for publication.*

0022-1767/05/$02.00

the C-terminal VWRPY motif, which mediates the interaction with Transducin-like enhancer of split (TLE), a transcriptional corepressor (22, 23) (see Fig. 3*A*), and a domain which represses *p21* transcription through the interaction with mammalian Sim3 isoform A corepressor (24) (not shown in Fig. 3*A*) are also known. Runx1 activates the transcription of different genes by interacting with different cofactors in various types of cells (25). To elucidate the mechanism by which Runx1 exerts various functions, the contributions of each domain to a particular function of Runx1 have been evaluated. Okuda et al. (26) examined the ability of full-length and mutant *Runx1* genes to rescue the hemopoietic defect in Runx1-deficient embryonic stem cells through a knock-in approach and demonstrated that the activation domain, but not the VWRPY motif, is indispensable for definitive hematopoiesis. No alterations in thymocyte subpopulations were detected in mice in which the VWRPY motif of Runx1 is genetically disrupted, although they have a significantly small thymus (27). In their study, the roles of the activation domain during thymocyte development were not assessed, due to a profound defect in hematopoiesis in the absence of the activation domain of Runx1. Therefore, the roles of functional domains of Runx1 in thymocyte development have not yet been adequately clarified.

Although fetal thymus organ culture (FTOC) has been conventionally used for in vitro studies on thymocyte development (28), it is difficult to achieve high gene-transduction efficiency and to obtain a sufficient number of cells for analyses with FTOC. We used an in vitro culture system in which fetal liver (FL) cells from wild-type mouse embryos follow normal thymocyte development on a layer of OP9-Delta-like 1 (DL1) murine stromal cells expressing a Notch ligand, DL1, on their surface (29, 30). In this system, FL cells from Runx1-deficient embryos exhibited defective thymocyte development, which was successfully restored by the reintroduction of full-length Runx1 by retroviral infection. We also introduced several forms of Runx1 mutants into the Runx1-deficient FL cells and evaluated their ability to restore thymocyte development, which revealed distinct functions of Runx1 domains during thymocyte development.

Materials and Methods

Preparation of cDNAs of Runx1 mutants and gene transduction

cDNAs of C-terminal deletion mutants of Runx1, Δ447, Δ372, Δ320, and Δ291, with a *NotI* site on their 5′ terminus and an *XhoI* site on their 3′ terminus, were PCR amplified from template murine *Runx1* cDNA (a gift from M. Satake, Tohoku University, Sendai, Japan) using *TaKaRa LA taq* (Takara Bio) with the following sets of primers: a sense oligonucleotide for all constructs, 5′-AAAAGCGGCCGCATCGATACCATGCGTATCCCC GT-3′; antisense oligonucleotides: *Δ477*, 5′-TTTTCTCGAGTCAGGC CTCCTCCAGGCGCGCGGG-3′; *Δ372*, 5′-TTTTCTCGAGTCAGCCGG TCTGGAAGGGCCCGGC-3′; *Δ320*, 5′-TTTTCTCGAGTCAGCGCGGG TCGGAGATGGACG-3′; and *Δ291*, 5′-TTTTCTCGAGTCAAAGTT CTGCAGAGAGGCTGG-3′. Each PCR product was digested with *NotI* and *XhoI* and cloned into the *NotI*-*XhoI* site, 5′ upstream of internal ribosomal entry site-*GFP* of the *pGCDNsam* (a gift from H. Nakauchi, Tokyo University, Tokyo, Japan) retrovirus vector (31). Nucleotide sequences of these mutant plasmids were confirmed using the ABI Ready Reaction Dye Terminator Cycle Sequencing kit and ABI3100 semiautomated sequencers (Applied Biosystems). To obtain retrovirus-producing cells, ψMP34 packaging cells (a gift from Wakunaga Pharmaceutical) were transfected with these retrovirus plasmids, followed by single cell sorting for GFP with a FACSVantage (BD Biosciences). To characterize cells transduced with retrovirus plasmids, GFP-positive cells were gated and analyzed.

Cell preparation and genotyping

Embryos at 14.5 days postcoitus (E14.5) were obtained by mating *Runx1*$^{+/-}$ mice (female) and *Runx1*$^{floxed/+}$, *Lck-Cre* transgenic (tg)$^{+}$ mice (male), both of which had been backcrossed for nine generations to C57BL/6. *Lck-Cre* tg mice were kindly provided by J. Takeda (Osaka University, Osaka, Japan) (32). FLs were dissected from the E14.5 embryos and then subjected to single cell suspension by pipetting. An aliquot of the FL cell suspension was subjected to DNA extraction followed by genotyping using PCR with primers *f2* (5′-ACAAAACCTAGGTGTAC CAGGAGAACAAGT-3′), *f120* (5′-CCCTGAAGACAGGAGAAGTTT CCA-3′), and *r1* (5′-GTCTACTCCTTGCCTCAGAAAACAAAAAC-3′), in which floxed and floxed-out (or deleted) alleles were amplified as 280-bp (f120-r1) and 220-bp (f2-r1) PCR fragments, respectively.

Culture of FL cells on OP9-DL1 stromal cells

FL cells were cultured on OP9-DL1 cells (generous gifts from J.C. Zúñiga-Pflücker, University of Toronto, Toronto, Canada) (29) according to the original descriptions with minor modifications. In brief, mononuclear cells were separated from a single cell suspension of E14.5 embryos of C57BL/6 mice by centrifugation on a Ficoll-Hypaque (AXIS-SHIELD; Lymphoprep) gradient. A total of 5×10^4 mononuclear cells, without further purification of hemopoietic progenitor cells, was cultured on confluent OP9-DL1 cells in flat-bottom 24-well culture plates with 500 μl of MEM (Invitrogen Life Technologies) supplemented with 20% FCS, penicillin/streptomycin, and 5 ng/ml recombinant human (rh) IL-7 (R&D Systems). After 5 days of culture, 5×10^4 cells were passed onto newly prepared OP9-DL1 cells in the presence of 5 ng/ml rhIL-7, and retrovirus infection was performed using polybrene (final concentration 8 μg/ml), followed by another 5 days of culture. A total of 1×10^5 cells were again passed onto newly prepared OP9-DL1 cells and cultured for another 5 days, but in rhIL-7-free culture medium.

Flow cytometry

Cells were collected from culture plates, suspended in PBS, and then incubated with mAbs for 30 min on ice. If necessary, this was followed by additional incubation with the secondary reagents for another 30 min on ice. After being washed with PBS, cells were analyzed by flow cytometry using a FACSCalibur (BD Biosciences) equipped with CellQuest software. All mAbs and fluorochromes used in flow cytometry were purchased from BD Pharmingen: FITC, PE, PerCP, PerCP-CY5.5, allophycocyanin, or Biotin-conjugated CD3ε (500A2), CD4 (RM4-5), CD8a (53-6.7), CD24 (M1/69), CD25 (PC61), CD44 (IM7), CD45.2 (104), CD45R/B220 (RA3-6B2), CD90.2 (Thy1.2: 52-2.1), or TCRβ (H57-597). Intracellular anti-TCRβ allophycocyanin staining was performed using a BD Cytofix/Cytoperm kit (BD Pharmingen) in accordance with the manufacturer's instructions.

Results

Normal FL cells can differentiate into DN and DP thymocytes on OP9-DL1 cells

The ontogenic profiles of nonpurified FL cells on OP9-DL1 cells were essentially similar to those of purified FL cells for hemopoietic progenitor cells (CD24^{low}, Lin$^-$, Sca-1^{high}, CD117/c-Kit$^+$) (29). Most of the FL cells from wild-type C57BL/6 mouse embryos cultured on OP9-DL1 cells expressed Thy1 without the distinct expression of B220, whereas FL cells cultured on parental OP9 cells did not show a high expression level of Thy1 but had apparently committed to B lymphocytes, as manifested by B220 expression (Fig. 1*A*). After 15 days of culture on OP9-DL1 cells, a considerable number of FL-derived cells became CD4$^+$CD8$^+$ (Fig. 1*B*) and were thought to correspond to CD4/8 DP thymocytes. These CD4$^+$CD8$^+$ cells also expressed TCRβ at a level comparable with that in DP thymocytes in adult thymus (Fig. 1*C*), indicating that the FL cells cultured on OP9-DL1 cells in vitro can follow the normal development of DP thymocytes in the thymus. A small number of SP (i.e., CD4$^+$CD8$^-$ or CD4$^-$CD8$^+$) cells were also observed, but they expressed only intermediate levels of TCRβ on their cell surface (Fig. 1*C*), suggesting that these cells were not as fully mature as the CD4 SP cells or the CD8 SP cells in the thymus. Another prevalent population in the normal FL cell culture on OP9-DL1 cells was CD4$^-$CD8$^-$ cells, which were considered to be reminiscent of CD4/CD8 DN thymocytes. DN thymocytes differentiate through the maturation sequences DN1 (CD44$^+$CD25$^-$), DN2 (CD44$^+$CD25$^+$), DN3 (CD44^{low}CD25$^-$), and DN4 (CD44$^-$CD25$^-$) (33), and each DN fraction was detected in FL-derived CD4$^-$CD8$^-$ cells cultured on OP9-DL1 cells

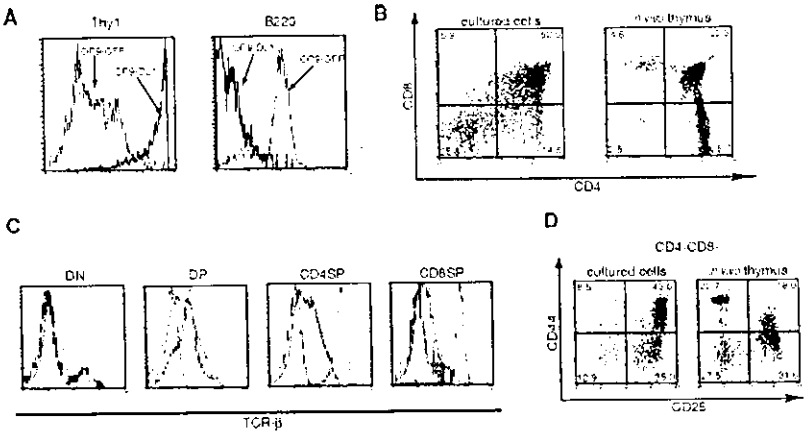

FIGURE 1. FACS analysis of wild-type C57BL/6 FL cells cultured on a stromal layer of OP9 cells that express DL1 (OP9-DL1). *A*, Expression levels of B220 and Thy1 on day 15 in FL cells cultured on an OP9-DL1 layer (thick line) and in FL cells cultured on a control OP9 layer (OP9-GFP; thin line) are shown. Cells were stained with anti-B220 PerCP and anti-Thy1.2 FITC. *B*, CD4/8 expression profile of FL cells cultured on OP9-DL1 for 15 days. The percentage of cells in each quadrant is indicated. *C*, FL cells cultured on OP9-DL1 for 15 days were stained with anti-CD4 PE, anti-CD8 PerCP, and anti-TCRβ allophycocyanin. Expression levels of TCRβ (filled histograms) in each subpopulation, as determined by CD4 and CD8 expression, are shown with the isotype control (blue lines) and expression levels of TCRβ in a corresponding population of adult thymocytes (red lines). *D*, Cells cultured on OP9-DL1 for 15 days were stained with anti-CD4 FITC, anti-CD44 PE, anti-CD8 PerCP, and anti-CD25 allophycocyanin. $CD4^-CD8^-$ cells were gated and their CD25/CD44 expression profile was analyzed. The percentage of cells in each quadrant is indicated.

by staining with CD25 and CD44, although the proportion of cells at the DN2 stage was prominent (Fig. 1*D*).

Phenotypes of Runx1 *conditionally knocked out (cko) FL cells cultured on OP9-DL1 cells*

Using this FL/OP9-DL1 coculture system, FL cells from *Runx1*-targeted (cko: $Runx1^{floxed/-}$, *Lck-Cre* tg) mice were tested for their capacity to differentiate into DP thymocytes. Whereas 10 days of culture of the control (ctrl; $Runx1^{+/+}$, *Lck-Cre* tg) FL cells on OP9-DL1 cells exclusively produced $CD4^-CD8^-$ cells, a similar culture of cko FL cells generated a population that showed an intermediate expression level of CD4 without CD8 ($CD4^{int}CD8^-$) in addition to $CD4^-CD8^-$ cells (Fig. 2*A*). The $CD4^{int}CD8^-$ subset in the cko FL cell culture is thought to be as immature as the $CD4^-CD8^-$ subset because it is quite unlikely that so many cko cells can differentiate beyond DP stage, due to that fact that only a small proportion of ctrl cells progressed to the $CD4^+CD8^+$ cells after 10 days of culture (Fig. 2*A*). Indeed, TCRβ and CD5, whose expression levels rise as thymocytes maturate, were up-regulated in $CD4^+CD8^+$ ctrl cells, but not in $CD4^+CD8^-$ cko cells (Fig. 2*B*). In addition, CD24, whose expression level diminishes as thymocytes maturate, is down-regulated in $CD4^+CD8^+$ ctrl cells, but not in $CD4^+CD8^-$ cko cells (Fig. 2*B*). Furthermore, the expression profile of CD44 and CD25 was comparable with that of $CD4^-CD8^-$ cells (Fig. 2*C*). The extent of Cre-mediated depletion of the floxed *Runx1* allele was greater in $CD4^{int}CD8^-$ cells than in the $CD4^-CD8^-$ cells (Fig. 2*D*), which is consistent with the fact that Runx1 actively represses *CD4* expression in DN thymocytes (14). After 15 days of culture, the ctrl FL cells cultured on OP9-DL1 cells consisted mainly of $CD4^+CD8^+$ and $CD4^-CD8^-$ cells, corresponding to DP and DN thymocytes in the thymus, respectively (Fig. 2*A*). In contrast, cko FL cells cultured for 15 days contained mainly $CD4^-CD8^-$ cells, and only a small fraction were $CD4^+CD8^+$ cells. The $CD4^+CD8^+$ cells from the ctrl FL cell culture showed higher expression levels of TCRβ than did $CD4^-CD8^-$ cells, whereas expression of TCRβ on $CD4^+CD8^+$ cells derived from cko FL cells was as low as that on $CD4^-CD8^-$ cells (data not shown), indicating the impaired maturation of $CD4^+CD8^+$ cells derived from cko FL cells on day 15. These observations are consistent with our unpublished finding in *Runx1* cko mouse, in which TCRβ expression on DP and CD4 SP thymocytes was significantly reduced.[4]

The DN ($CD4^-CD8^-$) population in the ctrl FL-derived cells appeared to contain four subsets of DN1 to DN4 on day 15 of culture (Fig. 2*E*). In contrast, the $CD4^-CD8^-$ population observed in the cko FL cell culture mainly consisted of DN1 and DN2 cells, indicating differentiation arrested at the DN2–3 transition. Thus, on OP9-DL1 cells, ctrl FL cells produced both DN and DP cells in almost the same manner as FL cells from wild-type C57BL/6 mice, whereas thymocyte development from cko FL cells was significantly impaired at the DN2–3 transition and showed the premature expression of CD4.

Runx1 gene transduction can restore the impaired differentiation of Runx1-deficient FL cells

To confirm that the impaired maturation of cko FL-derived cells was caused by a lack of Runx1, we examined whether the reintroduction of Runx1 could rescue the block in the DN2–3 transition found in cko FL-derived cells. The cko FL-derived cells transduced with *Runx1* by retrovirus infection showed a significant increase in DN3 cells accompanied by the appearance of DN4 cells, which was not seen in mock-infected cells (Fig. 3*B*, *top panel*). These results demonstrated that Runx1 is essential for the DN2–3 transition during thymocyte development. Remarkably, when Runx1 was introduced, the control FL cells generated more DN3 and DN4 cells than did mock-infected ctrl FL cells (Fig. 3*B*, *bottom panel*), suggesting that an increased dosage of Runx1 may also affect thymocyte development.

We next sought to determine the functional domains of Runx1 that are involved in thymocyte development. For this purpose, we generated a series of C-terminal deletion mutants of Runx1 (Fig. 3*A*) and transduced them into cko FL cells by retrovirus infection. Infection efficiencies were ~80% as assessed by GFP positivity and were almost constant for all of the constructs (data not shown). Δ447 lacks the C-terminal VWRPY motif, which is required for interaction with TLE (22, 23), whereas Δ372 lacks the inhibitory domain that impedes transcriptional activity mediated by the activation domain of Runx1 (21). The Δ320 mutant lacks a part of the

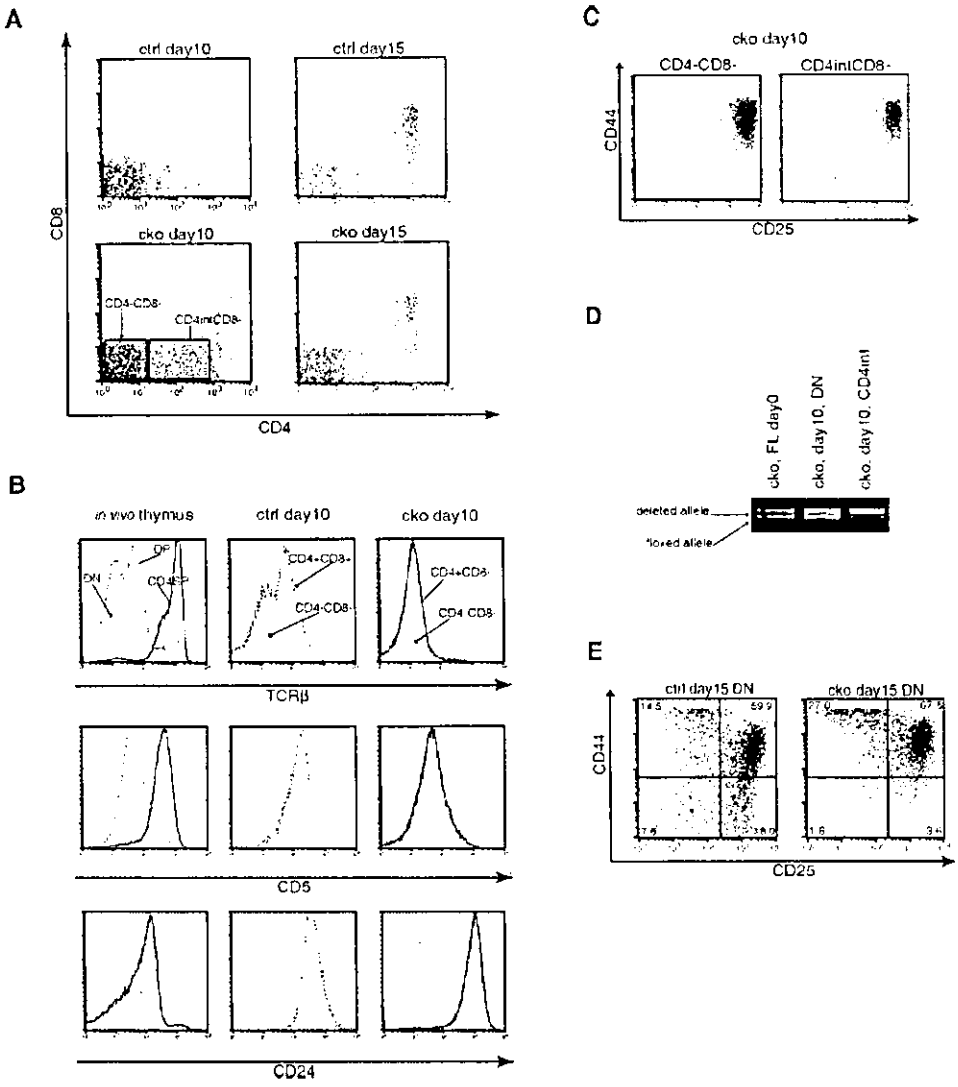

FIGURE 2. FACS analysis of cko FL cells and ctrl FL cells cultured on OP9-DL1. *A*, CD4/CD8 expression profiles of each type of FL-derived cell on days 10 and 15. *B*, Expression levels of TCRβ, CD5, and CD24 in $CD4^+CD8^-$ cko cells (solid lines) and $CD4^+CD8^+$ ctrl cells (dotted lines) cultured for 10 days were compared with those of $CD4^-CD8^-$ cells (gray shades without contour). Those for the indicated subsets of ctrl cells cultured for 10 days and thymocytes derived from adult thymus were also presented. *C*, CD25/CD44 expression profiles of $CD4^-CD8^-$ cells and $CD4^{int}CD8^-$ cells among cko FL cells cultured for 10 days. *D*, Genotype of each subpopulation of cko FL-derived cells, which were sorted with a FACSVantage SE cell sorter (BD Biosciences) after being stained with anti-CD4 PE and anti-CD8 PerCP-CY5.5. Genomic DNA was extracted from sorted cells and electrophoresed after amplification by PCR. *E*, CD25/CD44 expression profiles of $CD4^-CD8^-$ cells on day 15.

activation domain, and Δ291, which completely lacks the activation domain, shows less potent transcriptional activity than does Δ320 (21). The proportions of DN3 and DN4 cells on day 15 of culture were calculated for cko FL-derived cells infected with each mutant (Fig. 3*C*).

Δ*447*-transduced cko FL cells produced DN3 and DN4 cells in numbers comparable with full-length *Runx1*-transduced cko FL cells. Therefore, the VWRPY motif is not necessary for the function of Runx1 in the DN2–3 transition. Although Δ372, which lacks the inhibitory domain, can rescue the DN2–3 transition as efficiently as full-length Runx1, rescue of the DN3–4 transition was still marginally impaired. Despite the fact that the transcriptional activity of Runx1 is derepressed in the absence of the inhibitory domain (21), the differentiation of Δ*372*-transduced cko FL cells is not promoted compared with that of *Runx1*-transduced cko FL cells in this culture system, suggesting that the elevated transcriptional activity does not affect Runx1-dependent thymocyte development.

In contrast, both Δ320 and Δ291, which lack part of and the entire activation domain, respectively, failed to restore either the DN2–3 or DN3–4 transition. Thus, the activation domain is required for the function of Runx1 in the DN2–3 and DN3–4 transitions. Interestingly, the DN3 and DN4 subsets of Δ*320*- or Δ*291*-transduced control FL cells were diminished compared with mock-infected ctrl FL cells (Fig. 3*B*, *bottom panels*), which raises the possibility that both Δ320 and Δ291 suppress the function of endogenous Runx1 in the DN2–3 and DN3–4 transitions in a dominant-negative manner. The suppressive effects of Δ320 and Δ291 were confirmed in three independent experiments (proportions of DN3 cells, $p = 0.031$ for mock vs Δ320 and $p = 0.016$ for mock vs Δ291; proportions of DN4 cells, $p = 0.028$ for mock vs Δ320 and $p = 0.029$ for mock vs Δ291).

To determine the efficiency of Cre-mediated gene deletion in this culture system, genotyping of the *Runx1* alleles was performed for each stage of DN cells. DN3 and DN4 cells were obtained from day 10 culture of *Runx1*-transduced $Runx1^{floxed/floxed}$, *Lck-Cre* tg FL cells. The whole culture on day 5 was used to genotype DN2 cells, because almost all of the cells were at the DN2 stage on day 5. Genomic DNA was extracted from each DN subpopulation and used as a template for genotyping. Only the floxed allele was detected in the FL cells on day 0, whereas both the floxed and deleted alleles were detected in day 5 DN2 cells. In contrast, only the deleted allele was detected from the DN3 and DN4 subsets derived from *Runx1*-transduced FL cells (Fig. 3*D*). These results indicated that Cre-mediated gene deletion was only partially achieved in the DN2 cells, but was complete at the DN3 stage in this culture system.

Because our unpublished observation using *Runx1* cko mice revealed decreased TCRβ expression in Runx1-deficient DN3 thymocytes,[4] we examined expression of intracellular TCRβ in DN

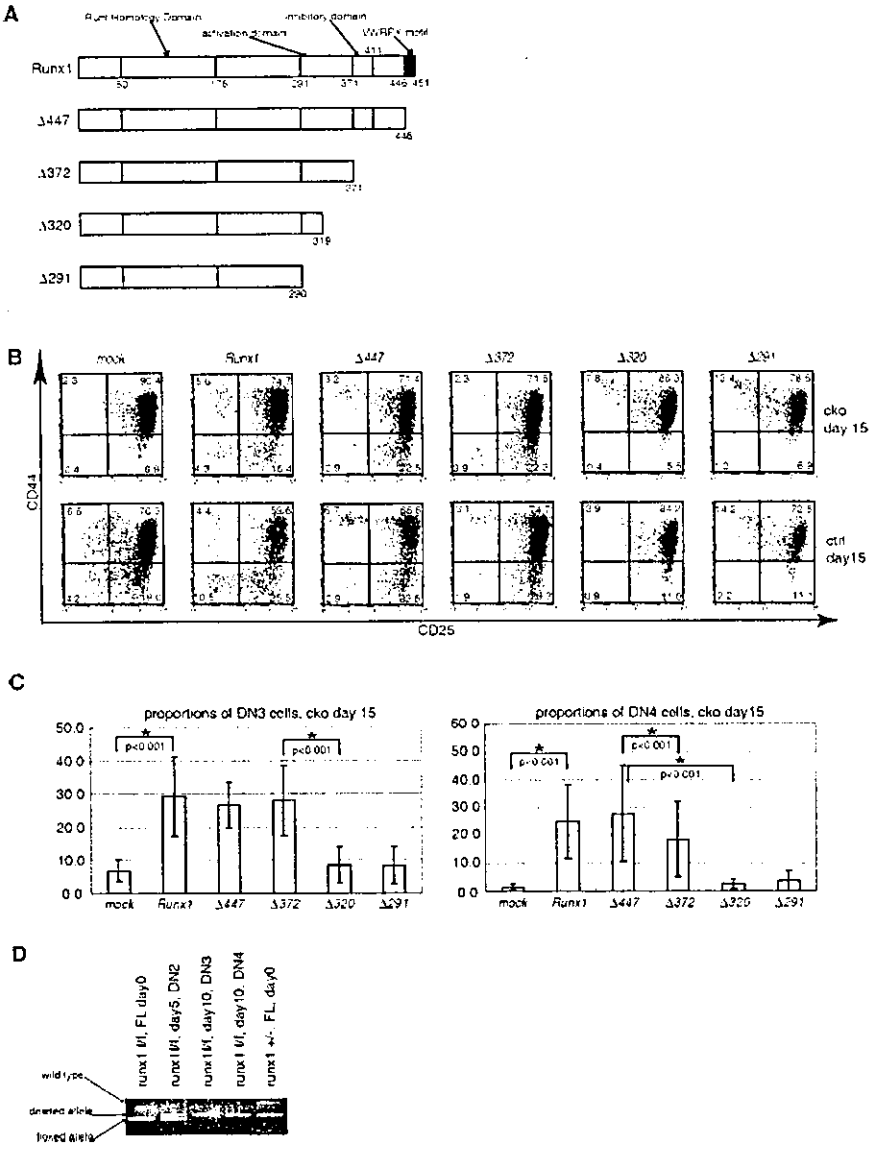

FIGURE 3. Development of DN3 and DN4 cells in FL-derived cells, which were transduced with the genes for Runx1 or its C-terminal deletion mutants. *A*, Construction of Runx1 and C-terminal deletion mutants. Numbers indicate the positions of amino acid residues from the N terminus. *B*, CD25/CD44 expression profile of CD4/CD8 DN cells on day 15 are shown for cko FL-derived cells (*top panels*) and ctrl FL-derived cells (*bottom panels*) with transduced Runx1 mutants. Cells were stained with anti-CD44 PE, anti-CD3 PerCP, anti-CD4 PerCP, anti-CD8 PerCP, and anti-CD25 allophycocyanin. GFP-positive and PerCP-negative cells were gated and analyzed for the CD25/CD44 expression profile. The percentage of cells in each quadrant is indicated. *C*, Proportions (%) of DN3 ($CD44^{low}CD25^{+}$) and DN4 ($CD44^{-}CD25^{-}$) cells on day 15 in nine independent experiments were averaged and are shown with ±1× SE. Asterisks indicate statistically significant differences, and *p* values were indicated. ANOVA and post hoc comparison (Fisher test) were performed using StatView software (SAS Institute). *D*, DN3 and DN4 thymocytes were sorted by a FACSVantage SE cell sorter (BD Biosciences) after being stained by anti-CD3ε PE, anti-CD4 PE, anti-CD8 PE, anti-CD25 PerCP-CY5.5, and anti-CD44 allophycocyanin. Genomic DNA was extracted from the sorted cells and electrophoresed after PCR amplification.

cells in day 15 culture of FL cells. A significant proportion of *Runx1*-transduced cko DN cells expressed intracellular TCRβ, whereas TCRβ was barely detected in mock-infected cko DN cells (Fig. 4). Transduction of *Δ447* or *Δ372* restored intracellular TCRβ expression to a level comparable with that of full-length *Runx1*, whereas cko DN cells transduced with *Δ320* or *Δ291* did not express intracellular TCRβ. In accordance with the increase in the proportions of DN3 and DN4 cells among *Runx1*-transduced ctrl cells (Fig. 3*B*, *bottom*), the percentage of *Runx1*-transduced ctrl DN cells expressing intracellular TCRβ was increased compared with the

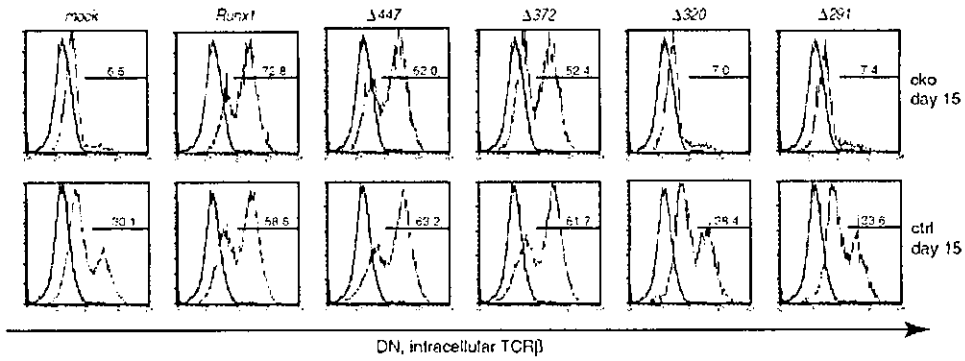

FIGURE 4. Expression levels of intracellular TCRβ in the $CD4^{-}CD8^{-}$ subset among cko (*top panels*) and ctrl (*bottom panels*) FL-derived cells on day 15. Transduced Runx1 mutants are shown above. Cells were stained with anti-CD4 PE, anti-CD8 PerCP, and anti-TCRβ allophycocyanin. GFP-positive, PE-negative, and PerCP-negative cells were analyzed for TCRβ expression (filled histograms). Expression levels of intracellular TCRβ in splenic B cells are overlaid as negative controls (thick lines). The percentages of positive cells are indicated in each histogram.

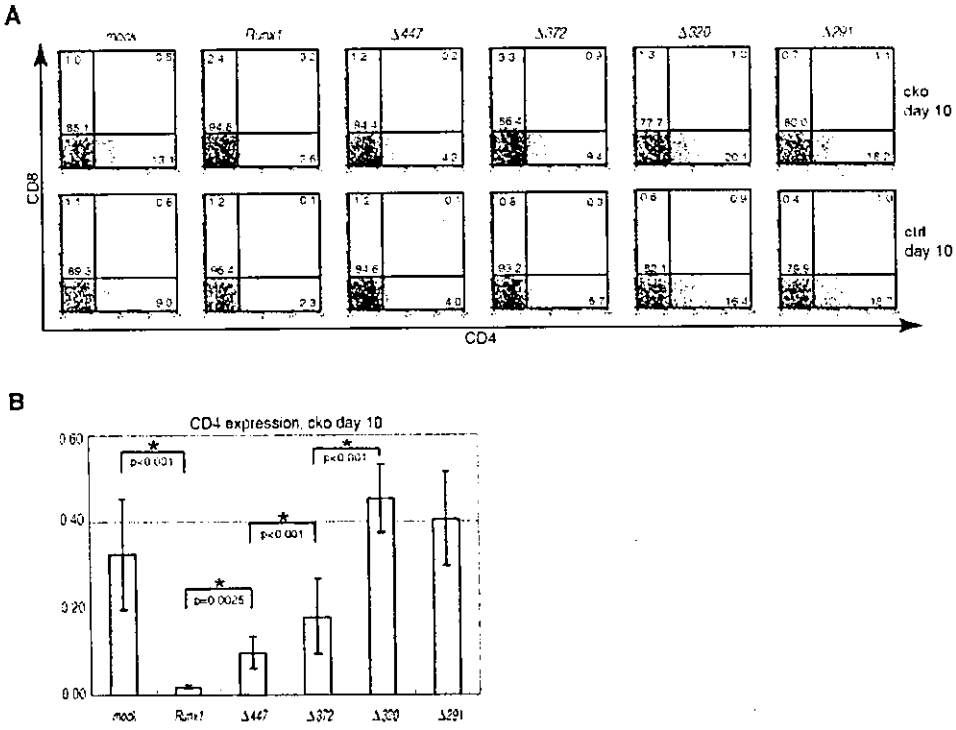

FIGURE 5. CD4 repression in the FL-derived cells transduced with Runx1 or its C-terminal deletion mutants. *A*, $CD4^-CD8$ expression profiles of cko (*top panels*) and ctrl (*bottom panels*) FL cells on day 10 of culture. Transduced Runx1 mutants are shown above. Cells were stained with anti-CD4 PE, anti-CD8 PerCP, and anti-CD45.2 allophycocyanin. GFP-positive and allophycocyanin-positive cells were analyzed for CD4/8 expression. The percentage of cells in each quadrant is indicated. *B*, Proportions (%) of $CD4^{int}$ cells among CD8-negative cells in nine independent experiments were averaged and are shown with ±1× SE. ANOVA and post hoc comparison (Fisher test) were performed using StatView software (SAS Institute). Asterisks indicate the statistically significant differences, and *p* values were indicated.

mock-infected cells (Fig. 4, *bottom*), and those TCRβ-expressing cells corresponded with CD44-negative (DN3 or DN4) cells (data not shown). Although it is yet to be determined whether decreased expression of TCRβ was the cause or the result of impaired thymocyte differentiation, the fact that the *TCRβ* gene has canonical binding sites for Runx1 within its enhancer region (34) and is transcriptionally up-regulated by Runx1 (8) supports the notion that Runx1 promotes thymocyte maturation at least partly by up-regulating TCRβ expression. Our results also indicate that the activation domain, but not the VWRPY motif, is critical for Runx1-mediated TCRβ up-regulation.

C-terminal VWRPY motif of Runx1 is necessary for CD4 repression

As shown in Fig. 5*A*, the $CD4^{int}CD8^-$ subsets in day 10 culture of cko FL cells disappeared upon the reintroduction of *Runx1* (Fig. 5*A*), which was again consistent with the established role of Runx1 in *CD4* repression (14). This observation also demonstrates that the aberrant expression of CD4 observed in DN subsets of cko FL-derived cells can be ascribed to *Runx1* depletion. To determine the domains of Runx1 that are relevant for CD4 repression, a series of C-terminal deletion mutants of Runx1 were transduced into cko or ctrl FL cells, and the proportion of $CD4^{int}CD8^-$ cells was evaluated on day 10 of culture (Fig. 5). Whereas full-length Runx1 almost completely repressed aberrant CD4 expression, only partial repression was seen with Δ447 or Δ372 mutants. These results suggest that CD4 repression by Runx1 requires some C terminus-mediated interaction with other molecules such as TLE. The extent of CD4 repression by Δ447 is greater than that by Δ372, which might reflect the existence of an additional repression domain in the C terminus other than the VWRPY motif (23).

Δ320 and Δ291 each failed to repress CD4 expression, resulting in an increase in the $CD4^{int}$ population compared with the mock-infected cko FL cells. Because *Runx1* depletion is incomplete in the DN subsets of cko FL-derived cells on day 10 (Fig. 2*D*), the increase in the $CD4^{int}$ population is probably due to a dominant-negative effect of Δ320 and Δ291 on remaining endogenous Runx1. This notion is supported by the observation that *Δ320*- or *Δ291*-transduced control FL cells produced a significant number of $CD4^{int}CD8^-$ cells, which were barely detected in mock-infected ctrl FL-derived cells (Fig. 5*A*, *bottom*).

Discussion

In the current study, we demonstrated that Runx1 was important for thymocyte development using the FL/OP9-DL1 coculture system. This system is superior to conventional FTOC in that a sufficient number of cells for extensive analyses can be easily obtained, especially DN thymocytes. Another advantage of this system is the highly efficient transfer of the genes of interest. In this study, we were able to introduce various mutants of Runx1 by retroviral infection with an efficiency of ~80% (data not shown), which is higher than that obtained with FTOC. In contrast, terminal maturation of SP cells cannot be achieved in this culture system, which makes it difficult to analyze more mature stages of thymocytes.

The absolute need for Runx1 in thymocyte development in vivo has been unequivocally demonstrated using conditionally *Runx1*-targeted mice. When Runx1-deficient bone marrow cells are transplanted to lethally irradiated mice, the development of thymocytes is severely blocked at the DN2–3 transition (35), whereas the deletion of *Runx1* in later stages of DN thymocytes using the *Lck-Cre* tg results in a profound defect in the DN3–4 transition.[4] Together, these findings suggest that Runx1 is necessary for normal thymocyte development at multiple steps during the DN-DP transition. Despite the DN3–4 block in T lymphocyte-specific *Runx1*-targeted mice, thymocyte development of the cognate FL cells was arrested at the DN2–3 transition in this culture system. The difference in the DN stage at which the developmental block occurs may be due to earlier Cre-mediated *Runx1* deletion in vitro rather than in vivo. In the FL culture system, deletion of the floxed *Runx1* allele occurs predominantly at the DN2–3 transition, which leaves few, if any, DN3 cells with an intact *Runx1* allele (Fig. 3*D*, *lane 3*). *Lck-Cre* tg mice harbor a transgenic gene encoding Cre recombinase driven by the $p56^{lck}$ proximal promoter (32, 36). The *Lck*

encodes a lymphocyte-specific protein tyrosine kinase, which mediates β-chain-dependent signaling during β-selection, is associated with allelic exclusion of β locus (37), and is transcribed from two developmentally regulated, independently functioning promoters. The proximal promoter is used exclusively in thymocytes, but not in peripheral T lymphocytes (38), and Cre-mediated gene deletions are expected to be activated by $p56^{lck}$ proximal promoter at the DN2 and DN3 stages when Vβ gene rearrangement and subsequent β-selection occurs. However, even if the same $p56^{lck}$ proximal promoter is used, exact timing of gene expression differs depending on the transgenic mice lines, and different lines of *Lck-Cre* tg mice are used to target a gene at different developmental stages (39).

The function of the VWRPY motif in hematopoiesis has been examined in embryonic stem cell culture (26) and in para-aortic splanchnopleural culture (40). Because Runx1 mutants that lack the VWRPY motif could fully restore hematopoiesis in Runx1-deficient cells in these two studies, the VWRPY motif does not seem to be necessary for hematopoiesis. On the contrary, because mice in which cDNA for the VWRPY-deficient Runx1 mutant had been homozygously knocked-in to the *Runx1* alleles exhibited a reduced number of thymocytes and deviant CD4 expression during thymocyte ontogeny (27), the VWRPY motif seems to play a role in thymocyte development, although the precise molecular mechanism is unclear. In the present study, although the VWRPY-deficient Runx1 mutant (Δ447) could restore not only maturation to the DN4 subset but also TCRβ expression in cko FL-derived thymocytes as efficiently as wild-type Runx1 (Fig. 4), it had only a limited capacity to repress aberrant CD4 expression (Fig. 5). These different requirements for the VWRPY motif indicate that Runx1 functions in both TLE-dependent and TLE-independent manners during early thymocyte development. In fact, the context-dependent need for interaction with a transcriptional corepressor has been reported for Runt and Groucho, *Drosophila* homologues of Runx and TLE, respectively (41). One possible explanation for TLE-dependent *CD4* repression is that TLE actively converts Runx1 to a transcriptional repressor by recruiting histone deacetylase, as seen in *Drosophila* (41). Another possibility is that TLE displaces some coactivators from Runx1 under particular conditions, which prevents Runx1 from up-regulating *CD4* expression. A similar mechanism has been proposed for transcription by lymphoid enhancer binding protein 1/T cell factor, which is repressed until TLE is replaced by β-catenin (42). Further analyses are needed to clarify the role of the VWRPY motif in the regulation of *CD4* transcription.

The introduction of Runx1 mutants into cko FL cells has shown that the activation domain makes a critical contribution to various functions of Runx1 in thymocyte development, including *CD4* repression, the DN2–3 transition, and the expression of TCRβ. Significantly, Δ320 and Δ291, both of which lack the activation domain, dominantly suppress *CD4* repression and the DN2–3 transition but do not interfere with TCRβ expression. This may be due to a higher affinity of Runx1 for the *TCRβ* enhancer compared with Δ320 and Δ291. Although this speculation is not supported by experimental evidence, a potential mechanism that accounts for this finding is that the interaction of Runx1 with other transcription factors may confer on Runx1 a higher affinity for specific gene promoters. Otherwise, Δ320 and Δ291 may retain a marginal potential to up-regulate TCRβ, which would prevent the total loss of TCRβ when they are forcibly expressed.

In conclusion, we have successfully reproduced the phenotype of Runx1-deficient thymocytes in vitro using the FL/OP9-DL1 coculture system and have evaluated the function of Runx1 and its mutants by retroviral gene transduction. The activation domain is essential for the function of Runx1 in *CD4* repression, the DN2–3 transition, and the expression of TCRβ, whereas the VWRPY motif does not contribute to the DN2–3 transition or the expression of TCRβ, but it is partially involved in *CD4* repression. Further studies are needed to understand how the VWRPY motif of Runx1 regulates *CD4* transcription and how Runx1 functions at multiple steps in thymocyte development.

Acknowledgments

We thank M. Satake for the gift of cDNA for murine *Runx1*, J.C. Zúñiga-Pflücker for OP9-DL1 stromal cells, H. Nakauchi for *pGCDNsam*, and Wakunaga Pharmaceutical for ψMP34 packaging cells. We also thank E. Nakagami-Yamaguchi and T. Yamagata for their helpful discussions.

Disclosures

The authors have no financial conflict of interest

References

1. Miyoshi, H., K. Shimizu, T. Kozu, N. Maseki, Y. Kaneko, and M. Ohki. 1991. t(8;21) breakpoints on chromosome 21 in acute myeloid leukemia are clustered within a limited region of a single gene, AML1. *Proc. Natl. Acad. Sci. USA 88:10431.*
2. Okuda, T., J. van Deursen, S. W. Hiebert, G. Grosveld, and J. R. Downing. 1996. AML1, the target of multiple chromosomal translocations in human leukemia, is essential for normal fetal liver hematopoiesis. *Cell 84:321.*
3. Wang, Q., T. Stacy, M. Binder, M. Marin-Padilla, A. H. Sharpe, and N. A. Speck. 1996. Disruption of the *Cbfa2* gene causes necrosis and hemorrhaging in the central nervous system and blocks definitive hematopoiesis. *Proc. Natl. Acad. Sci. USA 93:3444.*
4. Wang, S., Q. Wang, B. E. Crute, I. N. Melnikova, S. R. Keller, and N. A. Speck. 1993. Cloning and characterization of subunits of the T-cell receptor and murine leukemia virus enhancer core-binding factor. *Mol. Cell. Biol. 13:3324.*
5. Bae, S. C., Y. Yamaguchi-Iwai, E. Ogawa, M. Maruyama, M. Inuzuka, H. Kagoshima, K. Shigesada, M. Satake, and Y. Ito. 1993. Isolation of PEBP2 αB cDNA representing the mouse homolog of human acute myeloid leukemia gene, AML1. *Oncogene 8:809.*
6. Ogawa, E., M. Maruyama, H. Kagoshima, M. Inuzuka, J. Lu, M. Satake, K. Shigesada, and Y. Ito. 1993. PEBP2/PEA2 represents a family of transcription factors homologous to the products of the Drosophila runt gene and the human AML1 gene. *Proc. Natl. Acad. Sci. USA 90:6859.*
7. Giese, K., C. Kingsley, J. R. Kirshner, and R. Grosschedl. 1995. Assembly and function of a TCRα enhancer complex is dependent on LEF-1-induced DNA bending and multiple protein-protein interactions. *Genes Dev. 9:995.*
8. Sun, W., B. J. Graves, and N. A. Speck. 1995. Transactivation of the Moloney murine leukemia virus and T-cell receptor β-chain enhancers by cbf and ets requires intact binding sites for both proteins. *J. Virol. 69:4941.*
9. Hernandez-Munain, C., and M. S. Krangel. 1995. c-Myb and core-binding factor/PEBP2 display functional synergy but bind independently to adjacent sites in the T-cell receptor δ enhancer. *Mol. Cell. Biol. 15:3090.*
10. Hernandez-Munain, C., and M. S. Krangel. 1994. Regulation of the T-cell receptor δ enhancer by functional cooperation between c-Myb and core-binding factors. *Mol. Cell. Biol. 14:473.*
11. Satake, M., S. Nomura, Y. Yamaguchi-Iwai, Y. Takahama, Y. Hashimoto, M. Niki, Y. Kitamura, and Y. Ito. 1995. Expression of the Runt domain-encoding PEBP2 α genes in T cells during thymic development. *Mol. Cell. Biol. 15:1662.*
12. Simeone, A., A. Daga, and F. Calabi. 1995. Expression of runt in the mouse embryo. *Dev. Dyn. 203:61.*
13. Woolf, E., C. Xiao, O. Fainaru, J. Lotem, D. Rosen, V. Negreanu, Y. Bernstein, D. Goldenberg, O. Brenner, G. Berke, D. Levanon, and Y. Groner. 2003. Runx3 and Runx1 are required for CD8 T cell development during thymopoiesis. *Proc. Natl. Acad. Sci. USA 100:7731.*
14. Taniuchi, I., M. Osato, T. Egawa, M. J. Sunshine, S. C. Bae, T. Komori, Y. Ito, and D. R. Littman. 2002. Differential requirements for Runx proteins in CD4 repression and epigenetic silencing during T lymphocyte development. *Cell 111:621.*
15. Hayashi, K., N. Abe, T. Watanabe, M. Obinata, M. Ito, T. Sato, S. Habu, and M. Satake. 2001. Overexpression of AML1 transcription factor drives thymocytes into the CD8 single-positive lineage. *J. Immunol. 167:4957.*
16. Komine, O., K. Hayashi, W. Natsume, T. Watanabe, Y. Seki, N. Seki, R. Yagi, W. Sukzuki, H. Tamauchi, K. Hozumi, et al. 2003. The Runx1 transcription factor inhibits the differentiation of naive $CD4^+$ T cells into the Th2 lineage by repressing GATA3 expression. *J. Exp. Med. 198:51.*
17. Mikhail, F. M., K. A. Serry, N. Hatem, Z. I. Mourad, H. M. Farawela, D. M. El Kaffash, L. Coignet, and G. Nucifora. 2002. A new translocation that rearranges the AML1 gene in a patient with T-cell acute lymphoblastic leukemia. *Cancer Genet. Cytogenet. 135:96.*
18. Mikhail, F. M., L. Coignet, N. Hatem, Z. I. Mourad, H. M. Farawela, D. M. El Kaffash, N. Farahat, and G. Nucifora. 2004. A novel gene, FGA7, is fused to RUNX1/AML1 in a t(4;21)(q28;q22) in a patient with T-cell acute lymphoblastic leukemia. *Genes Chromosomes Cancer 39:110.*
19. Bae, S. C., E. Ogawa, M. Maruyama, H. Oka, M. Satake, K. Shigesada, N. A. Jenkins, D. J. Gilbert, N. G. Copeland, and Y. Ito. 1994. PEBP2 αB/mouse

AML1 consists of multiple isoforms that possess differential transactivation potentials. *Mol. Cell. Biol. 14:3242.*

20. Tanaka, T., K. Tanaka, S. Ogawa, M. Kurokawa, K. Mitani, J. Nishida, Y. Shibata, Y. Yazaki, and H. Hirai. 1995. An acute myeloid leukemia gene, AML1, regulates hemopoietic myeloid cell differentiation and transcriptional activation antagonistically by two alternative spliced forms. *EMBO J. 14:341.*
21. Kanno, T., Y. Kanno, L. F. Chen, E. Ogawa, W. Y. Kim, and Y. Ito. 1998. Intrinsic transcriptional activation-inhibition domains of the polyomavirus enhancer binding protein 2/core binding factor α subunit revealed in the presence of the β subunit. *Mol. Cell. Biol. 18:2444.*
22. Imai, Y., M. Kurokawa, K. Tanaka, A. D. Friedman, S. Ogawa, K. Mitani, Y. Yazaki, and H. Hirai. 1998. TLE, the human homolog of groucho, interacts with AML1 and acts as a repressor of AML1-induced transactivation. *Biochem. Biophys. Res. Commun. 252:582.*
23. Levanon, D., R. E. Goldstein, Y. Bernstein, H. Tang, D. Goldenberg, S. Stifani, Z. Paroush, and Y. Groner. 1998. Transcriptional repression by AML1 and LEF-1 is mediated by the TLE/Groucho corepressors. *Proc. Natl. Acad. Sci. USA 95:11590.*
24. Lutterbach, B., J. J. Westendorf, B. Linggi, S. Isaac, E. Seto, and S. W. Hiebert. 2000. A mechanism of repression by acute myeloid leukemia-1, the target of multiple chromosomal translocations in acute leukemia. *J. Biol. Chem. 275:651.*
25. Kitabayashi, I., A. Yokoyama, K. Shimizu, and M. Ohki. 1998. Interaction and functional cooperation of the leukemia-associated factors AML1 and p300 in myeloid cell differentiation. *EMBO J. 17:2994.*
26. Okuda, T., K. Takeda, Y. Fujita, M. Nishimura, S. Yagyu, M. Yoshida, S. Akira, J. R. Downing, and T. Abe. 2000. Biological characteristics of the leukemia-associated transcriptional factor AML1 disclosed by hematopoietic rescue of AML1-deficient embryonic stem cells by using a knock-in strategy. *Mol. Cell. Biol. 20:319.*
27. Nishimura, M., Y. Fukushima-Nakase, Y. Fujita, M. Nakao, S. Toda, N. Kitamura, T. Abe, and T. Okuda. 2004. VWRPY motif-dependent and -independent roles of AML1/Runx1 transcription factor in murine hematopoietic development. *Blood 103:562.*
28. Kingston, R., E. J. Jenkinson, and J. J. Owen. 1985. A single stem cell can recolonize an embryonic thymus, producing phenotypically distinct T-cell populations. *Nature 317:811.*
29. Schmitt, T. M., and J. C. Zúñiga-Pflücker. 2002. Induction of T cell development from hematopoietic progenitor cells by δ-like-1 in vitro. *Immunity 17:749.*
30. Huang, E. Y., A. M. Gallegos, S. M. Richards, S. M. Lehar, and M. J. Bevan. 2003. Surface expression of Notch1 on thymocytes: correlation with the double-negative to double-positive transition. *J. Immunol. 171:2296.*
31. Suzuki, A., K. Obi, T. Urabe, H. Hayakawa, M. Yamada, S. Kaneko, M. Onodera, Y. Mizuno, and H. Mochizuki. 2002. Feasibility of ex vivo gene therapy for neurological disorders using the new retroviral vector GCDNsap packaged in the vesicular stomatitis virus G protein. *J. Neurochem. 82:953.*
32. Takahama, Y., K. Ohishi, Y. Tokoro, T. Sugawara, Y. Yoshimura, M. Okabe, T. Kinoshita, and J. Takeda. 1998. Functional competence of T cells in the absence of glycosylphosphatidylinositol-anchored proteins caused by T cell-specific disruption of the Pig-a gene. *Eur. J. Immunol. 28:2159.*
33. Godfrey, D. I., J. Kennedy, T. Suda, and A. Zlotnik. 1993. A developmental pathway involving four phenotypically and functionally distinct subsets of $CD3^-CD4^-CD8^-$ triple-negative adult mouse thymocytes defined by CD44 and CD25 expression. *J. Immunol. 150:4244.*
34. Krimpenfort, P., R. de Jong, Y. Uematsu, Z. Dembic, S. Ryser, H. von Boehmer, M. Steinmetz, and A. Berns. 1988. Transcription of T cell receptor β-chain genes is controlled by a downstream regulatory element. *EMBO J. 7:745.*
35. Ichikawa, M., T. Asai, T. Saito, G. Yamamoto, S. Seo, I. Yamazaki, T. Yamagata, K. Mitani, S. Chiba, H. Hirai, S. Ogawa, and M. Kurokawa. 2004. AML-1 is required for megakaryocytic maturation and lymphocytic differentiation, but not for maintenance of hematopoietic stem cells in adult hematopoiesis. [Published erratum appears in *2005 Nat. Med. 11:102.*] *Nat. Med. 10:299.*
36. Hennet, T., F. K. Hagen, L. A. Tabak, and J. D. Marth. 1995. T-cell-specific deletion of a polypeptide *N*-acetylgalactosaminyl-transferase gene by site-directed recombination. *Proc. Natl. Acad. Sci. USA 92:12070.*
37. Anderson, S. J., and R. M. Perlmutter. 1995. A signaling pathway governing early thymocyte maturation. *Immunol. Today 16:99.*
38. Allen, J. M., K. A. Forbush, and R. M. Perlmutter. 1992. Functional dissection of the lck proximal promoter. *Mol. Cell. Biol. 12:2758.*
39. Bender, T. P., C. S. Kremer, M. Kraus, T. Buch, and K. Rajewsky. 2004. Critical functions for c-Myb at three checkpoints during thymocyte development. *Nat. Immunol. 5:721.*
40. Goyama, S., Y. Yamaguchi, Y. Imai, M. Kawazu, M. Nakagawa, T. Asai, K. Kumano, K. Mitani, S. Ogawa, S. Chiba, M. Kurokawa, and H. Hirai. 2004. The transcriptionally active form of AML1 is required for hematopoietic rescue of the AML1-deficient embryonic para-aortic splanchnopleural (P-Sp) region. *Blood 104:3558.*
41. Wheeler, J. C., C. VanderZwan, X. Xu, D. Swantek, W. D. Tracey, and J. P. Gergen. 2002. Distinct in vivo requirements for establishment versus maintenance of transcriptional repression. *Nat. Genet. 32:206.*
42. Roose, J., M. Molenaar, J. Peterson, J. Hurenkamp, H. Brantjes, P. Moerer, M. van de Wetering, O. Destree, and H. Clevers. 1998. The Xenopus Wnt effector XTcf-3 interacts with Groucho-related transcriptional repressors. *Nature 395:608.*

GENES, CHROMOSOMES & CANCER 42:269–279 (2005)

Identification of a SRC-Like Tyrosine Kinase Gene, *FRK*, Fused with *ETV6* in a Patient with Acute Myelogenous Leukemia Carrying a t(6;12)(q21;p13) Translocation

Noriko Hosoya,[1] Ying Qiao,[1] Akira Hangaishi,[1] Lili Wang,[1] Yasuhito Nannya,[1] Masashi Sanada,[1] Mineo Kurokawa,[1] Shigeru Chiba,[1,2] Hisamaru Hirai,[1,2] and Seishi Ogawa[1,3]*

[1]Department of Hematology and Oncology, Graduate School of Medicine, University of Tokyo, Tokyo, Japan
[2]Department of Cell Therapy and Transplantation Medicine, University of Tokyo Hospital, University of Tokyo, Tokyo, Japan
[3]Department of Regeneration Medicine for Hematopoiesis, Graduate School of Medicine, University of Tokyo, Tokyo, Japan

The SRC family of kinases is rarely mutated in primary human tumors. We report the identification of a SRC-like tyrosine kinase gene, *FRK* (Fyn-related kinase), fused with *ETV6* in a patient with acute myelogenous leukemia carrying t(6;12)(q21;p13). Both reciprocal fusion transcripts, *ETV6/FRK* and *FRK/ETV6*, were expressed. In *ETV6/FRK*, exon 4 of *ETV6* was fused in-frame to exon 3 of *FRK*, producing a chimeric protein consisting of the entire oligomerization domain of ETV6 and the kinase domain of FRK. The ETV6/FRK protein was shown to be constitutively autophosphorylated on its tyrosine residues. ETV6/FRK phosphorylated histones H2B and H4 in vitro to a greater extent than did FRK, suggesting it had elevated kinase activity. ETV6/FRK could transform both Ba/F3 cells and NIH3T3 cells, which depended on its kinase activity. Moreover, ETV6/FRK inhibited ETV6-mediated transcriptional repression in a dominant-negative manner. This report provides the first evidence that a SRC-like kinase gene, *FRK* fused with *ETV6*, could directly contribute to leukemogenesis by producing an oncoprotein, ETV6/FRK, with dual functions: constitutive activation of the ETV6/FRK tyrosine kinase and dominant-negative modulation of ETV6-mediated transcriptional repression. © 2004 Wiley-Liss, Inc.

INTRODUCTION

The *SRC* gene was the first protooncogene isolated as the cellular homologue of v-*SRC*, the retroviral transforming oncogene of avian Rous sarcoma virus (Brown and Cooper, 1996). Since then, it has become clear that *SRC* is the prototype for a family of genes that encode nonreceptor tyrosine kinases implicated in a variety of cellular processes, including cell growth, differentiation, and carcinogenesis. The SRC family of kinases shares common structures consisting of an N-terminal unique domain, SRC homology 3 (SH3) and SRC homology 2 (SH2) domains, a kinase domain, and a short C-terminal regulatory tail (Brown and Cooper, 1996). They are normally maintained in an inactive state through phosphorylation of a critical C-terminal tyrosine residue (Tyr 530 in human SRC, Tyr 527 in chicken SRC) by the C-terminal SRC kinase (Csk) (Brown and Cooper, 1996). The SH3 and SH2 domains also participate in this negative regulation through intramolecular interactions (Brown and Cooper, 1996; Schindler et al., 1999; Xu et al., 1999; Young et al., 2001).

The SRC and its family member kinases have long been postulated to participate in oncogenic processes. Activated variants of SRC family kinases, including the viral oncoprotein v-SRC, are capable of inducing malignant transformation in a variety of cell types (Parker et al., 1984; Cartwright et al., 1987). Activation of SRC-like kinases recently was described in *BCR-ABL1*-expressing acute lymphoblastic leukemia in mice (Hu et al., 2004). Elevated expression and/or activity of SRC have been documented in several types of primary human tumors (Bolen et al., 1987; Ottenhoff-Kalff et al., 1992; Talamonti et al., 1993). However, for many years, structural abnormalities of the SRC family of kinases have been detected rarely in primary human tumors. Although Irby et al. (1999)

Supported by: Research on Human Genome and Tissue Engineering, Health and Labour Sciences Research Grants, Ministry of Health, Labour and Welfare of Japan; Japan Society for the Promotion of Science; Grant number: KAKENHI 14570962.

*Correspondence to: Seishi Ogawa, Department of Hematology and Oncology, Department of Regeneration Medicine for Hematopoiesis, Graduate School of Medicine, University of Tokyo, 7-3-1, Hongo, Bunkyo-ku, Tokyo 113-8655, Japan.
E-mail: sogawa-tky@umin.ac.jp

Received 22 July 2004; Accepted 15 October 2004
DOI 10.1002/gcc.20147
Published online 20 December 2004 in Wiley InterScience (www.interscience.wiley.com).

reported that 12% of advanced human colon cancers had a truncating mutation at codon 531 of the *SRC* gene, determining the importance of this mutation in the generation of colorectal cancers remained elusive according to the negative results in subsequent reports (Daigo et al., 1999; Wang et al., 2000; Laghi et al., 2001). In primary hematopoietic malignancies, no studies have demonstrated structural abnormalities of the SRC family of kinases.

In this study, we performed molecular analysis of a t(6;12)(q21;p13) observed as the sole chromosomal abnormality in a case of acute myelogenous leukemia (AML) and identified a SRC-like tyrosine kinase gene, *FRK* (Fyn-related kinase or *Rak*), on 6q21 (Cance et al., 1994; Lee et al., 1994) that is fused with *ETV6* (also called *TEL*), a gene frequently involved in chromosomal translocations in a variety of human leukemias (Golub et al., 1997). We found that the resultant chimeric protein, ETV6/FRK, is a transforming oncoprotein with elevated kinase activity. We also demonstrated that ETV6/FRK inhibits ETV6-mediated transcriptional repression in a dominant-negative manner, indicating that ETV6/FRK is a unique oncoprotein with dual functions. This is the first report showing the involvement of a SRC-like kinase gene (*FRK*) in primary human cancers.

MATERIALS AND METHODS

Case History

The patient was a 69-year-old Japanese woman with AML-M4, carrying the translocation t(6;12)(q21;p13) as the sole chromosomal abnormality in 8 of 20 examined bone marrow metaphase cells. After obtaining informed consent, a sample of her bone marrow was taken for use in this study. The patient did not respond to chemotherapy and died 5 months later.

Fluorescence In Situ Hybridization Analysis

Fluorescence in situ hybridization (FISH) analysis was performed as previously described (Pinkel et al., 1986) with a panel of biotin- and digoxigenin-labeled cosmid probes that contained different exons of *ETV6*, kindly provided by Dr. Peter Marynen (University of Leuven, Leuven, Belgium). The order and the relative locations of cosmids are depicted in Figure 1A.

3′-Rapid Amplification of cDNA End

To do the 3′-rapid amplification of cDNA end (RACE), total RNA was isolated from the leukemic sample as described previously (Ogawa et al., 1996). First-strand cDNA was synthesized from 2.5 μg of total RNA using the primer R2N6 as described previously by Peeters et al. (1997). The first polymerase chain reaction (PCR) was performed with primers T4F1 and R2N6R1 (Peeters et al., 1997). Then, a diluted product of the first PCR, along with primers T4F2 and R2N6R2, was used for the second, nested PCR (Peeters et al., 1997). The nucleotide sequences of the primers used in this study and the conditions for PCR are listed in Table 1. The PCR products were subcloned into the pCR® 2.1-TOPO® vector using a TOPO TA Cloning® kit (Invitrogen, Tokyo, Japan) and subjected to DNA sequencing by use of a 3100 Applied Biosystems automated sequencer (Applied Biosystems, Chiba, Japan).

Reverse Transcriptase–PCR

For the reverse transcriptase-PCR (RT-PCR), 5 μg of the total RNA was transcribed to cDNA with 2 units of Moloney murine leukemia virus reverse-transcriptase (MMLV-RT, Stratagene, La Jolla, CA) using a random hexamer. One-tenth of the synthesized cDNA was directed to PCR analysis. Primers T4F2 and FRK1198R were used to confirm the *ETV6/FRK* transcripts. The primers for detecting the reciprocal *FRK/ETV6* transcripts were FRK451F and TEL723R. For amplification of the wild-type *ETV6* and *FRK* transcripts, primers T4F2 and TEL723R and primers FRK808F and FRK1198R, respectively, were used. All the sequences of the RT-PCR products were verified by direct sequencing.

Plasmid Construction

Full-length *ETV6* cDNA tagged with a FLAG sequence at the 5′ end, a gift from Dr. Kinuko Mitani (Dokkyo University School of Medicine, Tochigi, Japan), was subcloned into the expression plasmid pME18S-neo (Invitrogen, San Diego, CA). A FLAG-tagged full-length *FRK* cDNA was isolated by RT-PCR from total RNA obtained from human placenta using primers *Eco*RI-FLAG-FRK and FRK-*Not*I-2058R and was cloned into pME18S-neo. The pME18S-neo-FLAG-ETV6/FRK vector was generated by replacement of the *Cla*I-*Not*I fragment of the pME18S-neo-FLAG-ETV6 vector with the *Cla*I-*Not*I fragment of *ETV6/FRK*, which was obtained by RT-PCR from the patient's bone marrow using primers TEL-*Cla*I-F and FRK-*Not*I-2058R, with subsequent digestion with *Cla*I and *Not*I. To construct a kinase-inactive mutant of ETV6/FRK, designated ETV6/FRK(K262R), a point mutation corresponding

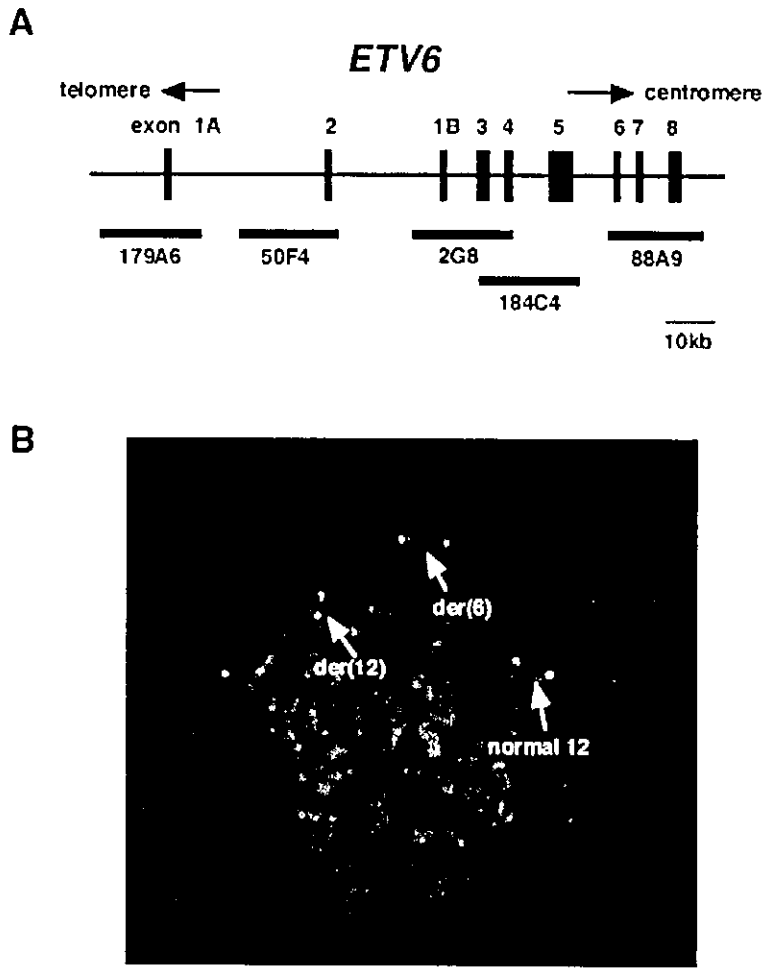

Figure 1. Analysis of breakpoint on chromosome 12. (A) A genomic map of *ETV6* and location of the cosmid probes used for FISH analysis. (B) FISH analysis of the patient's leukemic cells. The signals of the 2G8 probe (red) containing *ETV6* exons 1B, 3, and 4 are hybridized on the der(6) and on the normal 12p, whereas those of the 184C4 probe (green) containing *ETV6* exons 3–5 are found on the der(6), the der(12), and the normal 12p.

to a kinase-inactivating mutation in the ATP-binding site lysine residue (Lys262) of FRK was introduced into *ETV6/FRK* cDNA. A mutated fragment generated by PCR using the mutagenic primer FRK-K262R-*Bam*HI and the primer TEL-*Eco*RI-FLAG was spliced together with a C-terminal partial fragment of *FRK* into pME18S-neo. A FLAG-tagged full-length *FRK/ETV6* cDNA was constructed into the pME18S-neo vector by assembling partial fragments from *ETV6* and *FRK* and a fragment spanning the *FRK/ETV6* junction generated by RT-PCR using primers FRK451F and TEL723R. All the constructs were sequenced to confirm the fidelity of the sequence and conservation of the reading frame at the site of fusion.

Cell Lines, Transfection, and Cell Transformation Studies

For transient expression studies, 4×10^4 HeLa cells were seeded in each 60-mm dish and transfected with expression plasmid or plasmids 24 hr later by a lipofection method using Effectine™ Transfection Reagent (Qiagen, Hilden, Germany). Cells were incubated for 48 hr and harvested for analysis. NIH3T3 cells were transfected with expression plasmids, also using Effectine™, and selected in 400 μg/ml of G418 for 2 weeks. Ba/F3 clones stably expressing ETV6/FRK or other proteins were obtained by electroporation of each expression plasmid into Ba/F3 cells as previously described (Carroll et al., 1996) and subsequent isolation of individual G418-resistant subclones by limiting dilution. Expression of the transfected genes was evaluated by immunoblotting as previously described (Maki et al., 1999) using anti-FLAG-M2 monoclonal antibody (Sigma-Aldrich, St. Louis, MO). The soft-agar colony assay was performed as previously described (Kurokawa et al., 1996). After 21 days, all macroscopic colonies larger than 0.25 mm in diameter were counted. For growth curves, 2×10^4 G418-resistant Ba/F3 cells were washed 3 times with PBS and plated in IL-3-free medium on day 0, and viable cells were counted each day by trypan blue exclusion.

TABLE I. Primers Used For 3'-RACE and (RT)-PCR Amplifications

Name	Sequence
R2N6	5'-CCAGTGAGCAGAGTGACGAGGACTCGAGCTCAAGC(N)6-3'
T4F1	5'-CATATTCTGAAGCAGAGGAAA-3'
R2N6R1	5'-CCAGTGAGCAGAGTGACG-3'
T4F2	5'-ACACAGCCGGAGGTCATACT-3'
R2N6R2	5'-GAGGACTCGAGCTCAAGC-3'
FRK1198R	5'-CTTCCCATACTTCGCAAAC-3'
FRK451F	5'-AGCAACATCTGTCAGAGGCT-3'
TEL723R	5'-GTAGGACTCCTGGTGGTTGTT-3'
FRK808F	5'-ATCGGAAGATCAGATGCAGAG-3'
*Eco*RI-FLAG-FRK	5'-GCGAATTCGTTGTGATGGGGGACTACAAGGACGAC GATGACAAGTCCGGGAGCAACATCTGTCAGAGGCT-3'
FRK-*Not*I-2058R	5'-ATTGCGGCCGCACTGATTGTGCAGTTGGTTGA-3'
TEL-*Cla*I-F	5'-CTTTCGCTATCGATCTCCTCA-3'
TEL-*Eco*RI-FLAG	5'-GCGAATTCGTTGTGATGGGGGACTACAAGGACGAC GATGACAAGTCCGGGTCTGAGACTCCTGCTCAGTG-3'
FRK-K262R-*Bam*HI	5'-TTGGATCCATTGAACCTGGTTTTAATGTTCTCACTG-3'

Thermal cycling profile was: 94°C for 2 min, followed by 35 cycles of 94°C for 1 min, 60°C for 1 min and 72°C for 2 min, with a final extension at 72°C for 10 min.

Immunoprecipitation, Immunoblotting, and Immune Complex Kinase Assay

Lysates were prepared by washing cells (1×10^6–1×10^7) with phosphate-buffered saline and then adding lysis buffer [10 mM Tris-HCl (pH 7.4), 150 mM NaCl, 1.0% NP-40, 1 mM EDTA, and 1 mM Na3VO4] containing 5 mM phenylmethyl-sulfonylfluoride and 1 μg/ml of aprotinin. After 10 min on ice, the samples were centrifuged at 12,000 g to remove insoluble particles. For immunoprecipitation, 1 mg of total cell lysate was incubated with anti-FLAG-M2 antibody for 1 hr at 4°C, after which 50 μl of Protein G-Sepharose beads (Amersham Biosciences, Uppsala, Sweden) was added. After rotating for 1 hr at 4°C, immunoprecipitates were washed 3 times and boiled in loading buffer for 5 min. Protein samples were separated on 6.5%–15% gradient SDS-polyacrylamide gels and transferred onto PVDF membranes (Millipore, Bedford, MA). Immunoblotting was performed as previously described (Maki et al., 1999) using either anti-FLAG-M2 antibody or antiphosphotyrosine monoclonal antibody 4G10 (Upstate Biotechnology Incorporated, Lake Placid, NY) as a primary antibody.

For the immune complex kinase assay, immunoprecipitates were washed 3 times and suspended in kinase buffer [40 mM HEPES (pH 7.4), 10 mM $MgCl_2$, 5 mM $MnCl_2$]. For determination of kinase activity, 2.5 μg of either histone H2B or histone H4 (Roche Diagnostics K. K., Tokyo, Japan) was added to each reaction. Kinase reactions were initiated by the addition of 10 μCi of [γ-^{32}P] ATP (3,000 Ci/mmol; Amersham Biosciences Corp., Piscataway, NJ) and incubated at 30°C for 15 min. Reactions were stopped by the addition of loading buffer and analyzed by SDS-PAGE and exposure to a film.

Luciferase Assay

For the luciferase assay, 4×10^4 HeLa cells were transfected with 1 μg of the reporter plasmid (EBS)3tkLuc (Waga et al., 2003), a kind gift of Dr. Kinuko Mitani, along with the indicated amounts of the expression vectors. The total amount of DNA in weight was adjusted to be equal by adding pME18S-neo plasmid. Luciferase activities were determined as described previously (Maki et al., 1999). All transfection experiments were performed in duplicate at least 3 times.

RESULTS

Identification of the Breakpoint on Chromosome 12

We performed FISH experiments using several probes from the *ETV6* locus, on 12p13 (Fig. 1A). The signals from the cosmids containing exons 1–4 (179A6, 50F4, and 2G8) were found on the der(6) (Fig. 1B), whereas the signals from the cosmid containing exons 3–5 (184C4) were split to the der(6) and the der(12) (Fig. 1B), suggesting that the breakpoint on 12p13 was localized to *ETV6* exons 4–5. The signals on the normal 12p were always observed with all the indicated cosmid probes of the *ETV6* locus, suggesting that the non-

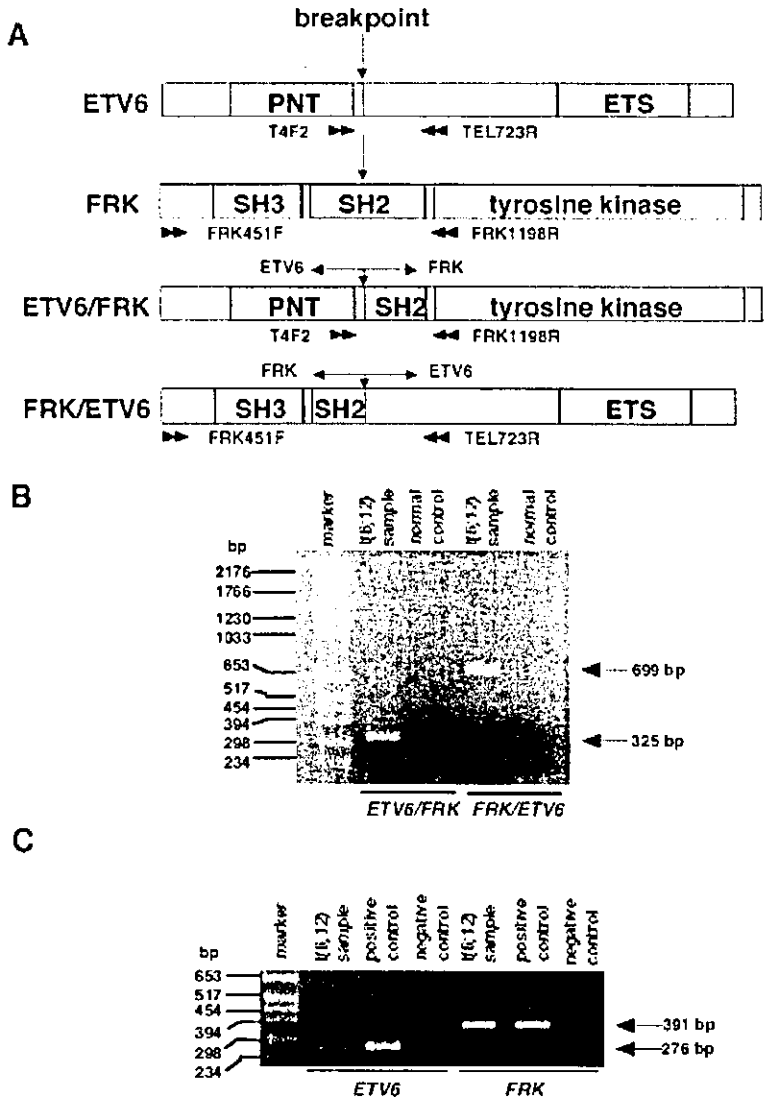

Figure 2. Identification of *ETV6/FRK* and *FRK/ETV6* fusion transcripts. (A) Schematic representation of wild-type *ETV6*, *FRK*, and the fusion transcripts. The breakpoints are indicated by vertical arrows. Horizontal arrows indicate the positions of RT-PCR primers (described in the Materials and Methods section). (B) Detection of *ETV6/FRK* as well as *FRK/ETV6* fusion transcripts by RT-PCR in the patient's leukemic sample. (C) Expression of *ETV6* and *FRK* in the patient's leukemic sample by RT-PCR.

translocated allele of *ETV6* was grossly intact with no large deletions.

Identification of the Fusion Partner of *ETV6*

To identify the unknown fusion partner of *ETV6*, 3′-RACE-PCR was performed. After two rounds of PCR, 3′-RACE-PCR products were successfully obtained. Sequencing analysis of the PCR products showed that exon 4 of *ETV6* was fused to exon 3 of *FRK* on 6q21, creating an *ETV6/FRK* fusion gene. The *FRK* gene encodes a SRC-like nonreceptor tyrosine kinase, consisting of the N-terminal SH3 and SH2 domains, the C-terminal kinase domain, and a short regulatory tail (Fig. 2A). The *ETV6/FRK* fusion gene produced a chimeric protein in which the entire pointed (PNT) oligomerization domain (also called helix–loop–helix domain) of ETV6 and the kinase domain of FRK were fused in-frame (Fig. 2A).

Detection of the *ETV6/FRK* and *FRK/ETV6* Fusion Transcripts

RT-PCR analysis was performed to confirm the fusion transcripts of the *ETV6* and *FRK* genes. Both reciprocal fusion transcripts, *ETV6/FRK* and *FRK/ETV6*, were specifically amplified from the leukemic sample but not from control bone marrow (Fig. 2B). Expression of wild-type *ETV6* and *FRK* also was detected in the leukemic sample (Fig. 2C). There were no mutations in the entire coding sequences of *ETV6*, *FRK*, *ETV6/FRK*, and *FRK/ETV6* (data not shown).

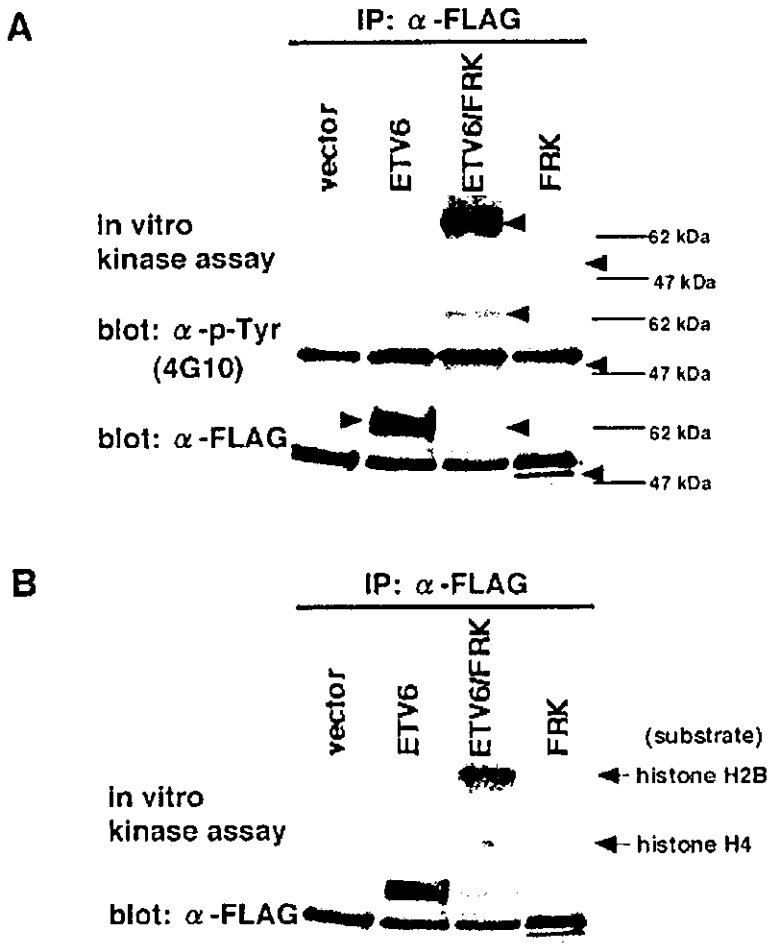

Figure 3. The ETV6/FRK tyrosine kinase is constitutively activated in HeLa cells. (A) Lysates of HeLa cells transfected with the indicated expression vectors were immunoprecipitated with an anti-FLAG-M2 monoclonal antibody and then analyzed by immune complex kinase assay (top) or immunoblotting with an antiphosphotyrosine antibody 4G10 (middle). The total amount of each protein was also assessed by immunoblotting with anti-FLAG-M2 antibody (bottom). Arrowheads show the proteins expressed or phosphorylated at an expected size. (B) Results of kinase assay performed with histones H2B (top) and H4 (middle).

Constitutive Activation of the ETV6/FRK Tyrosine Kinase

Because the ETV6/FRK fusion protein retained the kinase domain but lacked the SH3 domain and most of the SH2 domain, we examined its kinase activity. First, we compared the autophosphorylation status of ETV6/FRK and wild-type FRK. Either the ETV6/FRK fusion protein, wild-type FRK, or wild-type ETV6 FLAG-tagged at the N-terminus was introduced into HeLa cells, immunoprecipitated with an anti-FLAG-M2 monoclonal antibody, and then analyzed by the kinase assay or immunoblotting with an antiphosphotyrosine antibody 4G10 (Fig. 3A, top and middle). To compare expression levels, the same amounts of immunoprecipitate were also subjected to anti-FLAG blot (Fig. 3A, bottom). A high level of tyrosine phosphorylation occurred only in the ETV6/FRK protein (Fig. 3A, top and middle). A basal level of autophosphorylation also was detectable in the wild-type FRK (Fig. 3A, top), a finding in agreement with the previous data (Cance et al., 1994). However, the level of autophosphorylation was significantly lower than that of ETV6/FRK (Fig. 3A, top and middle). Next, we compared the ability of ETV6/FRK and wild-type FRK to phosphorylate exogenous substrates. When histone H2B or H4 was added to the kinase reaction, they were found to be phosphorylated to a greater extent in ETV6/FRK-expressing cells than in FRK-expressing cells (Fig. 3B), suggesting that the ETV6/FRK protein had elevated tyrosine kinase activity.

Cell Transformation by ETV6/FRK in a Kinase-Dependent Manner

To assay the transforming activities of ETV6/FRK, we stably expressed the cDNA-encoding ETV6/FRK or other proteins into the fibroblast cell line NIH3T3. We established 3 NIH3T3 clones expressing ETV6/FRK, 2 clones expressing FRK/ETV6, 2 clones expressing FRK, 2 clones expressing ETV6, and 2 clones expressing ETV6/FRK(K262R) (Fig. 4A), the kinase-inactive

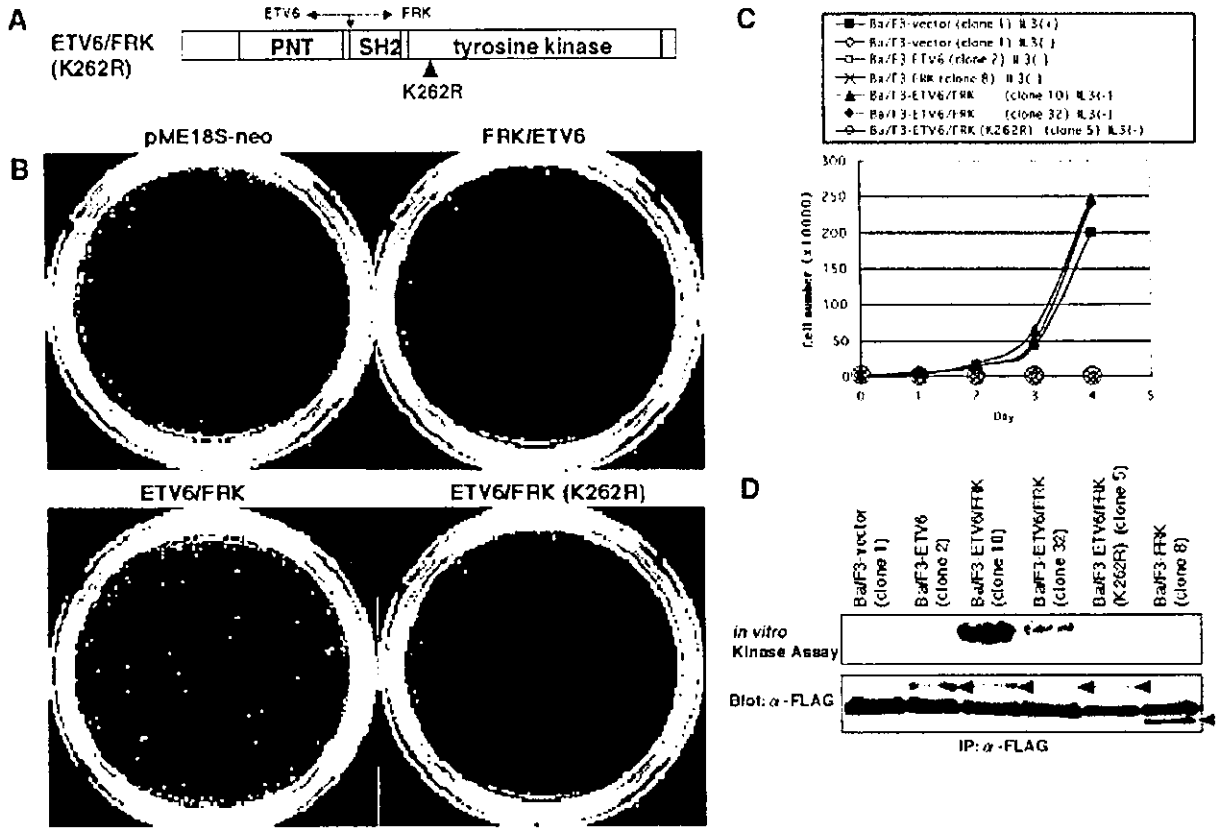

Figure 4. ETV6/FRK transforms NIH3T3 cells and Ba/F3 cells in a kinase-dependent manner. (A) Schematic representation of the kinase-inactive ETV6/FRK(K562R) mutant with a lysine-to-arginine mutation at the ATP binding site. (B) Soft-agar assay demonstrating macroscopic colony formation in ETV6/FRK-expressing NIH3T3 cells. (C) 2 × 10^4 Ba/F3 cells stably transfected with the indicated expression vectors were washed free of IL-3 and plated on day 0 in growth medium without IL-3. Viable cells were counted each day. Data of the representative clone(s) for each protein are presented. (D) Cell lysates of the indicated Ba/F3 clones were immunoprecipitated with an anti-FLAG-M2 antibody and then subjected to kinase assay (top) and immunoblotting with anti-FLAG-M2 antibody (bottom). Arrowheads show the proteins expressed at an expected size.

mutant of ETV6/FRK, confirmed by immunoblotting analysis (data not shown). The soft-agar assay was performed on each clone. Comparable results were obtained for the clones expressing the same proteins, and the representative data are presented. Only the NIH3T3 cells expressing intact ETV6/FRK were able to produce macroscopic colonies, whereas the NIH3T3 cells transfected with the empty vector or cells expressing the kinase-inactive mutant ETV6/FRK(K262R), the reciprocal FRK/ETV6 fusion protein, wild-type FRK, or wild-type ETV6 failed to grow colonies (Fig. 4B, Table 2). These results suggest that ETV6/FRK but not FRK/ETV6 contributes to neoplastic transformation in a kinase-dependent manner.

Next, we also examined the ability of ETV6/FRK to transform the murine hematopoietic cell line Ba/F3, which is strictly dependent on IL-3 for survival and proliferation. Following stable transduction by electroporation, we obtained 6 Ba/F3 clones expressing ETV6/FRK, 2 clones expressing FRK, 2 clones expressing ETV6, and 3 clones expressing ETV6/FRK(K262R), confirmed by immunoblotting analysis (data not shown). To assay the ability to confer independent proliferation of IL-3, each Ba/F3 clone was switched to growth medium without IL-3. Comparable results were obtained for the clones expressing the same proteins, and the representative data are presented. The Ba/F3 clones expressing ETV6/FRK showed sustained proliferation in the absence of IL-3 (Fig. 4C). In contrast, Ba/F3 cells transfected with the empty vector or cells expressing kinase-inactive mutant ETV6/FRK(K262R), wild-type FRK, and wild-type ETV6 were all unable to proliferate in the absence of IL-3 (Fig. 4C). Although the ETV6/FRK proteins expressed in the stable clones were constitutively autophosphorylated, the ETV6/FRK(K262R) mutants were not (Fig. 4D). These observations indicate that ETV6/FRK is a dominant oncoprotein and that constitutive activa-

TABLE 2. Transformation of NIH3T3 Cells By ETV6/FRK

Transfected DNA	No. of colonies[a]
pME18S-neo (vector)	0
pME18S-neo-ETV6	0
pME18S-neo-FRK	0
pME18S-neo-ETV6/FRK	15
pME18S-neo-ETV6/FRK(K262R)	0
pME18S-neo-FRK/ETV6	0

NIH3T3 cells were transfected with the indicated constructs, and stable transfectants were selected in G418. Cells were plated in soft agar. Macroscopic colonies were counted at day 21.
[a]Average of four experiments.

tion of the ETV6/FRK tyrosine kinase is necessary for ETV6/FRK-induced transformation.

Inhibition of ETV6-Mediated Transcription Repression by ETV6/FRK

Because ETV6 is an ETS transcription factor that acts as a transcriptional repressor (Lopez et al., 1999), we also investigated the transcriptional regulatory property of ETV6/FRK and its ability to modulate the function of wild-type ETV6. We transfected a previously described (EBS)3tkLuc reporter, in which the luciferase gene is placed under the control of an ETS responsive promoter (Waga et al., 2003), along with either wild-type ETV6, ETV6/FRK, or FRK/ETV6 into HeLa cells and evaluated luciferase activity. The results showed, in agreement with the previous finding (Waga et al., 2003), that there was decreased luciferase activity after cotransfection of (EBS)3tkLuc with the wild-type ETV6 expression plasmid (Fig. 5A). In contrast, no repression was observed when ETV6/FRK or FRK/ETV6 was expressed with the (EBS)3tkLuc reporter (Fig. 5A).

Because the oncoprotein ETV6/FRK lacks the ETS DNA binding site but still retains the PNT oligomerization domain, it is possible that it might affect ETV6-mediated transcriptional repression by heterodimerizing with ETV6. Notably, coexpression of ETV6/FRK abolished the transcriptional repression by ETV6 in a dose-dependent manner (Fig. 5B), suggesting that ETV6/FRK has a dominant-negative effect on ETV6-mediated transcriptional repression. In contrast, coexpression of the reciprocal FRK/ETV6 protein did not affect ETV6-mediated transcriptional repression (Fig. 5B). In control experiments, dose-dependent expression of the ETV6, ETV6/FRK, or FRK/ETV6 protein was confirmed by immunoblotting analysis (data not shown).

DISCUSSION

The t(6;12)(q21;p13) is a rare but recurrent reciprocal chromosome translocation in human leukemia (Hayashi et al., 1990; Katz et al., 1991; Raimondi et al., 1997). In this article, we report our finding that it generated novel fusion genes *ETV6/FRK* and *FRK/ETV6* in a case of AML. FRK belongs to a family of SRC kinases, as at the amino acid level, it has the highest homology, 50%, with FYN (Cance et al., 1994; Lee et al., 1994). Although several tyrosine kinase (TK) genes have been identified as fusion partners of *ETV6* (Golub et al., 1994; Papadopoulous et al., 1995; Lacronique et al., 1997; Peeters et al., 1997; Cazzaniga et al., 1999; Eguchi et al., 1999; Iijima et al., 2000; Kuno et al., 2001), this is the first report of a SRC-family tyrosine kinase gene being fused with *ETV6* and structurally altered in human cancers. In the resultant ETV6/FRK fusion protein, the entire PNT oligomerization domain of ETV6 and the kinase domain of FRK are fused in frame. We demonstrated that this ETV6/FRK fusion protein constitutively underwent autophosphorylation on its tyrosine residues. ETV6/FRK had elevated kinase activity compared to that in wild-type FRK. ETV6/FRK showed transforming activities in two cell lines, Ba/F3 and NIH3T3, indicating that ETV6/FRK is a dominant transforming oncoprotein. The kinase-inactive mutant ETV6/FRK(K262R) transformed neither of these two cell lines, indicating that the kinase activity of ETV6/FRK was essential for transformation. The reciprocal fusion protein FRK/ETV6, whose mRNA also was transcribed in the patient sample, did not have transforming activity. These data strongly suggest that the elevated kinase activity of the ETV6/FRK fusion protein directly contributes to the pathogenesis of leukemia with a t(6;12)(q21;p13).

Although activated variants of the SRC family kinases show transforming activities (Parker et al., 1984; Cartwright et al., 1987), the *SRC* and its family of genes rarely have been reported as being mutated or structurally altered in primary human tumors. Irby et al. (1999) reported that 12% of advanced human colon cancers in the United States had a truncating mutation at codon 531 of the *SRC* gene and that the mutation elevated kinase activity and promoted the potential for malignancy. However, three subsequent large-scale studies on advanced colorectal cancers in Japanese, northern European, Chinese, and Italian patients failed to detect the mutation (Daigo et al., 1999; Wang et al., 2000; Laghi et al., 2001), making the

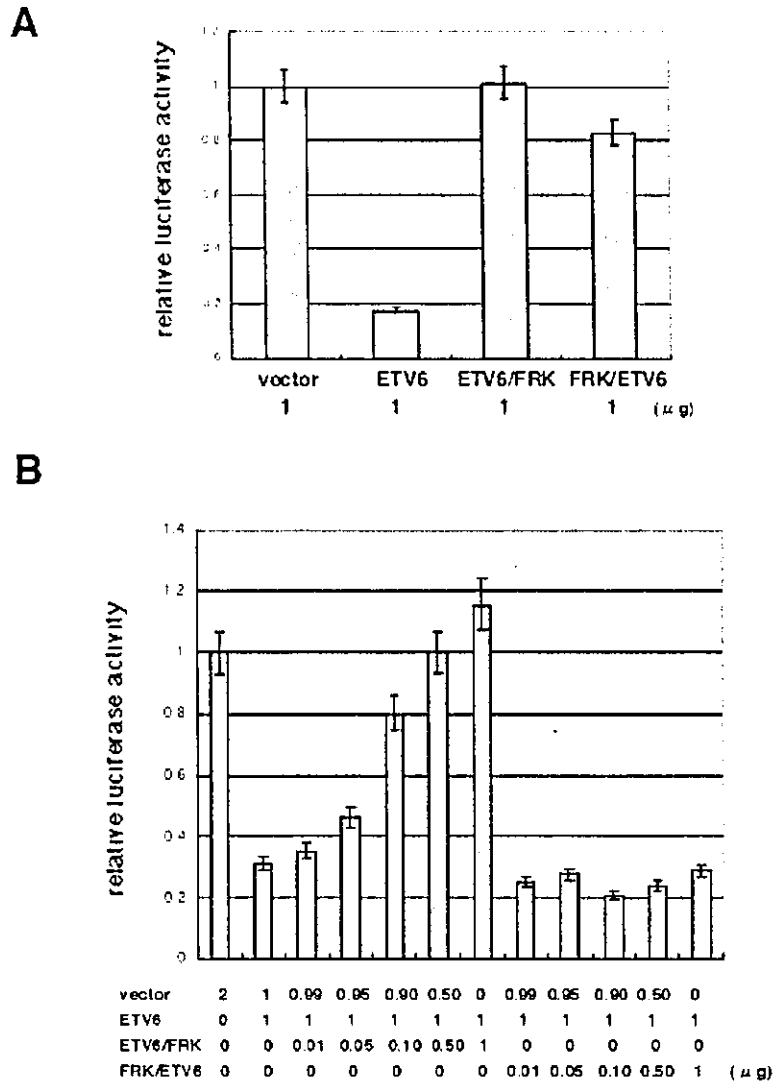

Figure 5. ETV6/FRK is a dominant-negative regulator of ETV6-mediated transcriptional repression in HeLa cells. (A) HeLa cells were transfected with 1 μg of (EBS)3tkLuc reporter plasmid along with 1 μg of the indicated expression vector. Bars show relative luciferase activities to the level when a control plasmid pME18S-neo was cotransfected with the corresponding reporter plasmid, and they present average results of duplicate experiments. (B) HeLa cells were transfected with 1 μg of (EBS)3tkLuc reporter plasmid along with 1 μg of pME-18S-neo-FLAG-ETV6 expression vector together with indicated amounts of pME18S-neo-FLAG-ETV6/FRK or pME18S-neo-FLAG-FRK/ETV6 expression vector. The results are presented as relative luciferase activities.

importance of this mutation controversial. In hematopoietic malignancies, two human T-cell acute lymphoblastic leukemia cell lines have been shown to have rearrangement of *LCK*, a SRC-family kinase gene (Tycko et al., 1991; Wright et al., 1994). In these two cell lines, HSB-2 and SUP-T12, the upstream promoter of the *LCK* gene was juxtaposed to the *TCRB* locus without any accompanying large structural abnormality of the LCK protein. *LCK* mRNA was elevated in the two cell lines (Tycko et al., 1991), and the HSB-2 cell line was later shown to carry several activating point mutations in the *LCK* gene (Wright et al., 1994), indicating that overexpression and/or activation of the LCK kinase would lead to cell transformation. On the other hand, the involvement of SRC family members in primary leukemia has not been reported previously. In this study, we showed that the structural abnormality, of an SRC-like kinase gene, *FRK*, through translocation with *ETV6* can directly contribute to leukemogenesis through activation of the altered tyrosine kinase. In addition to the analysis of the current case with a t(6;12), we also performed a mutation analysis of the *FRK* gene in 20 hematopoietic cell lines but failed to detect activating mutations or structural abnormalities (data not shown). Thus, it is currently unclear whether FRK could be activated through other mechanisms such as activating mutations or translocations with other partner gene(s), although more intensive analyses may be required.

Two mechanisms could contribute to the constitutive activation of the ETV6/FRK kinase. First, in the ETV6/FRK fusion protein, the SH3 and SH2 domains of FRK are lost or disrupted, respec-